European Journal of Operational Research 235 (2014) 115–128

Contents lists available at ScienceDirect

European Journal of Operational Research

journal homepage: www.elsevier.com/locate/ejor

Discrete Optimization

Exact algorithms for the traveling salesman problem with draft limits

Maria Battarra [a,*], Artur Alves Pessoa [b], Anand Subramanian [c], Eduardo Uchoa [b]

[a] University of Southampton, School of Mathematics, Southampton SO17 1BJ, UK
[b] Universidade Federal Fluminense, Departamento de Engenharia de Produção, Rua Passo da Pátria 156, Bloco E, 4° andar, São Domingos, Niterói, RJ 24210-240, Brazil
[c] Universidade Federal da Paraíba, Departamento de Engenharia de Produção, Centro de Tecnologia, Campus I, Bloco G, Cidade Universitária, João Pessoa, PB 58051-970, Brazil

ARTICLE INFO

Article history:
Received 20 February 2013
Accepted 15 October 2013
Available online 28 October 2013

Keywords:
Draft limits
Traveling salesman
Cutting planes
Column generation
Extended formulation

ABSTRACT

This paper deals with the Traveling Salesman Problem (TSP) with Draft Limits (TSPDL), which is a variant of the well-known TSP in the context of maritime transportation. In this recently proposed problem, draft limits are imposed due to restrictions on the port infrastructures. Exact algorithms based on three mathematical formulations are proposed and their performance compared through extensive computational experiments. Optimal solutions are reported for open instances of benchmark problems available in the literature.

1. Introduction

The Traveling Salesman Problem (TSP) with Draft Limits (TSPDL) is a variant of the well-known TSP, recently introduced by Rakke, Christiansen, Fagerholt, and Laporte (2012), that arises in the context of maritime transportation. The sequence of ports that a cargo ship visits in a tour is dependent on the port infrastructures: the sea-level in a port is sometimes not sufficiently deep to accommodate loaded cargo ships. The port is thus associated to a draft limit, i.e., the maximum vertical distance allowed between the waterline and the bottom of the hull. Note that the draft of a cargo ship depends on the load: the heavier the load, the higher the ship's draft. Therefore, draft limits can be easily translated into restrictions on the maximum load of the ship.

The problem can be formalized as follows: A directed graph $G = (V, A)$ is given, where $V = \{0, \ldots, n\}$ is the set of ports to be visited and $A = \{(i,j), i,j \in V, i \neq j\}$ is the arc set, or set of connections between ports. Each arc $(i,j) \in A$ is associated to a routing cost $c_{ij} > 0$. The vertex 0 is the port from which the ship starts and ends its tour, whereas vertices $V' = \{1, \ldots, n\}$ are ports to be visited exactly once. Each port requires the delivery of $d_i,\ i \in V'$, units of load and is associated to a draft limit $l_i,\ i \in V'$. The initial load is $Q = \sum_{i \in V'} d_i$ and we denote $\underline{d} = \min_{i \in V'}\{d_i\}$. The ship cannot enter port i if its load is heavier than l_i, or the hull of the ship could be grounded. Therefore the TSPDL asks for the minimum cost Hamiltonian tour, visiting each port exactly once and not violating draft limit constraints.

Despite its simple definition, the TSPDL proves hard to solve to optimality. In fact, the problem is $\mathcal{NP}$-Hard since it includes the TSP as special case when the drafts are sufficiently large.

Rakke et al. (2012) proposed two mathematical formulations: the first formulation makes use of the binary variables x_{ij} assuming value 1 if arc (i,j) is in the solution, and continuous variables y_{ij}, representing the load on the ship while traveling arc (i,j). The resulting formulation is compact, but provides poor quality bounds. The second formulation includes two additional sets of variables: u_j and t_{ij} specifying the position of port j and of arc (i,j) in the circuit, respectively. These two sets of variables allow for the introduction in the model of the Miller, Tucker, and Zemlin (MTZ) constraints (Miller, Tucker, & Zemlin, 1960). The MTZ constraints, usually employed to avoid subtours, are used to strengthen the formulation and they are included at the root node of the branch-and-bound tree.

Both formulations have been further strengthened by dynamically separating subtour elimination constraints (Dantzig, Fulkerson, & Johnson, 1954), as well as their lifted counterpart (Balas & Fischetti, 2004). Moreover, lower bounds on the u_j variables and lower bounds on the sum of y_{ij} variables are imposed.

The branch-and-cut algorithms originating from both formulations are capable of solving quite effectively instances with a limited amount of ports with draft limits, but when the percentage of ports with a draft limit increases, the algorithm struggles even for medium-sized instances. The problem seems therefore challenging and, as far as we are aware, no other attempts have been made to solve it exactly. This motivated our interest in the problem and we

* Corresponding author. Tel.: +44 (0)23 8059 3863.
E-mail addresses: m.battarra@soton.ac.uk (M. Battarra), artur@producao.uff.br (A.A. Pessoa), anand@ct.ufpb.br (A. Subramanian), uchoa@producao.uff.br (E. Uchoa).

0377-2217/$ - see front matter
http://dx.doi.org/10.1016/j.ejor.2013.10.042

decided to investigate alternative formulations and solution techniques.

Three alternative mathematical formulations are introduced (see Section 2). The first formulation is based on two-index variables, the second formulation is based on three-index variables, whereas the third can be viewed as an improvement over a Dantzig–Wolfe decomposition of the second, including the concept of *ng*-paths (Baldacci, Mingozzi, & Roberti, 2011), and it is solved through a branch-cut-and-price algorithm.

In Section 3, a description of the branch-and-cut and branch-cut-and-price implementations are presented. The results of our computational experience are summarized in Section 4, while Section 5 presents conclusions and future possible research directions.

2. Mathematical formulations

The exact algorithms proposed in this work are based on three integer programming formulations that are described in this section.

2.1. Formulation F1

The first formulation, denoted F1, is based on two sets of two-indexed binary variables. The x_{ij} variable assumes value 1 if $(i,j) \in A$ is in the solution, 0 otherwise. The variable y_{ik} assumes value 1 when the ship enters port $i \in V'$ carrying $k \in \{d_i, \ldots, l_i\}$ units of load, 0 otherwise. Note that arcs $(i,j) | d_j > l_i - d_i$ can be removed from the network: in order to simplify the notation we do not explicitly remove these arcs, but it is sufficient to disregard the corresponding variables in our models to take this aspect into account. The formulation F1 can be stated as follows:

$$(\text{F1}) \quad \min \sum_{(i,j)\in A} c_{ij} x_{ij} \tag{1}$$

$$\text{s.t.} \sum_{i \in V, i \neq j} x_{ij} = 1, \quad \forall j \in V \tag{2}$$

$$\sum_{j \in V, j \neq i} x_{ij} = 1, \quad \forall i \in V \tag{3}$$

$$\sum_{i \in V' | l_i \geqslant k} y_{ik} \leqslant 1, \quad \forall k \in \{\underline{d}, \ldots, Q - \underline{d}\} \tag{4}$$

$$\sum_{k=d_i}^{l_i} y_{ik} = 1, \quad \forall i \in V' \tag{5}$$

$$y_{iQ} = x_{0i}, \quad \forall i \in V' | l_i = Q \tag{6}$$

$$y_{id_i} = x_{i0}, \quad \forall i \in V' \tag{7}$$

$$x_{ij} + y_{ik} \leqslant 1 + y_{j,k-d_i}, \quad \forall (i,j) \in A, \quad k \in \{d_j + d_i, \ldots, \min\{l_i, l_j + d_i\}\} \tag{8}$$

$$x_{ij} \in \{0,1\}, \quad \forall (i,j) \in A \tag{9}$$

$$y_{ik} \in \{0,1\}. \quad \forall i \in V', k \in \{d_i, \ldots, l_i\} \tag{10}$$

The Objective Function (1) aims at minimizing routing costs. Constraints (2) and (3) are the degree constraints. Constraints (4) impose that the ship visits at most a port for each intermediate load value. Constraints (4) are not necessary to define an optimal integer solution, because Constraints (2), (3), (6) and (7) guarantee that the ship performs a Hamiltonian tour in which the load is monotonically decreasing. Preliminary experiments showed that these constraints strengthen the linear relaxation and we included them in the formulation. Constraints (5) state that each port has to be assigned to a load. The first and last position of the tour are imposed to be connected to the initial port 0 (Constraints (6) and (7), respectively). Constraints (8) link variables x_{ij} and y_{ik}: if arc (i,j) is traversed, $x_{ij} = 1$ and i and j are located in consecutive positions of the tour. Therefore summing variables x_{ij} and y_{ik} can result in a value equal to 2 only if $y_{j,k-d_i} = 1$. These constraints generalize similar constrains encountered in single-machine scheduling problems (an interested reader can refer to the models based on assignment and positional date variables in Keha, Khowala, & Fowler, 2009). Finally, Constraints (9) and (10) define the binary nature of the variables. Note that Constraints (5)–(8) ensure that the flow is monotonically decreasing along the tour and therefore subtours are avoided.

Formulation F1 presents similarities with the MTZ-based formulation for the *Asymmetric TSP* (ATSP) (see Roberti & Toth, 2012 for a recent overview and comparison of ATSP models), but consists only of binary variables.

F1 is strengthened by incorporating the trivial constraints

$$x_{ij} + x_{ji} \leq 1, \quad \forall (i,j) \in A \tag{11}$$

and by separating in a cutting plane fashion the subtour elimination constraints:

$$\sum_{i \in S} \sum_{j \in \bar{S}} x_{ij} \geqslant 1. \quad \forall S \subseteq V' \tag{12}$$

For this latter set of inequalities, the exact separation can be done in polynomial time.

2.2. Formulation F2

Formulation F2 considers three-indexed binary variables z_{ij}^k, assuming value 1 if arc $(i,j) \in A$ is traversed by the ship carrying k units of load (including the demand of port j). By denoting $K_{ij} = \min\{l_j, l_i - d_i\}$, formulation F2 is:

$$(\text{F2}) \quad \min \sum_{(i,j)\in A} \sum_{k=d_j}^{K_{ij}} c_{ij} z_{ij}^k \tag{13}$$

$$\text{s.t.} \sum_{\substack{i \in V \\ i \neq j}} \sum_{k=d_j}^{K_{ij}} z_{ij}^k = 1, \quad \forall j \in V \tag{14}$$

$$\sum_{\substack{j \in V | j \neq i \\ l_j \geqslant k + d_j}} z_{ji}^k - \sum_{\substack{j \in V | j \neq i \\ l_j \geqslant k - d_i, d_j \leqslant k - d_i}} z_{ij}^{k-d_i} = 0, \quad \forall i \in V, \quad k \in \{d_i, \ldots, l_i\} \tag{15}$$

$$z_{i0}^k = 0, \quad \forall i \in V', \quad k \in \{1, \ldots, Q\} \tag{16}$$

$$z_{0j}^k = 0, \quad \forall j \in V' | l_j = Q, \quad k < Q, \quad k \in \{d_j, \ldots, l_j\} \tag{17}$$

$$z_{ij}^k \in \{0,1\}. \quad \forall (i,j) \in A, \quad k \in \{d_j, \ldots, K_{ij}\} \tag{18}$$

The Objective Function (13) minimizes routing costs. Constraints (14) are the degree constraints. Constraints (15) preserve the load conservation. Constraints (16) and (17) force the ship to return to the depot empty and leave the depot carrying Q units, respectively. Constraints (18) define the nature of the variables. Formulation F2 is similar to the three-index formulations proposed in Fox, Gavish, and Graves (1980), for the *Time Dependent TSP*.

Constraints

$$\sum_{\substack{j \in V \\ j \neq i}} \sum_{k=d_j}^{K_{ij}} z_{ij}^k = 1, \quad \forall i \in V \tag{19}$$

are implied by Constraints (14) and Constraints (15), as previously stated in Pessoa, Poggi de Aragão, and Uchoa (2008).

F2 can be strengthened by the trivial constraints:

$$\sum_{k=d_j}^{K_{ij}} z_{ij}^k + \sum_{k=d_i}^{K_{ji}} z_{ji}^k \leqslant 1, \quad \forall (i,j) \in A \tag{20}$$

that have been included in the formulation *a priori*.

Flow conservation constraints ensure that subtours are avoided for F2 integer solutions, however we strengthened the formulation by including the subtour elimination constraints as cutting planes (as for F1):

$$\sum_{i\in S}\sum_{j\in\bar{S}}\sum_{k=d_j}^{K_{ij}} z_{ij}^k \geqslant 1, \quad \forall S \subseteq V' \tag{21}$$

Finally, F2 can be strengthened by adding the *2-cycle* inequalities:

$$z_{ij}^k \leqslant \sum_{\substack{t\in V, t\neq\{i,j\},\\ t|l_t \geqslant k-d_j}} z_{jt}^{k-d_j}, \quad (i,j)\in A, i,j\neq 0, \quad \forall k=\{d_j,\ldots,K_{ij}\} \tag{22}$$

as proposed in Abeledo, Fukasawa, Pessoa, and E. (2013). These constraints have been added to F2 in a cutting-plane fashion, using an exact enumerative separation procedure. Note that the constraints can be avoided for the arcs incident in the depot, because Constraints (16) and (17) ensure that no arcs return to the depot after visiting the first port and no arcs would visit a port after the depot.

Proposition 1. *The linear relaxation of F2 ((13)–(18)) dominates the linear relaxation of F1 ((1)–(10)).*

Proof. See Appendix. □

2.3. Formulation F3

F3 originates from an alternative interpretation of the solution space of F2, in the spirit of Pessoa et al. (2008). The left-side of Fig. 1 presents a TSPDL solution and the corresponding non-zero z_{ij}^k variables (the draft limits are 3, 3, and 1 for the ports 1, 2, and 3, respectively and each port asks for the delivery of one unit). The right side of the same figure pictures a path interpretation of the same solution. For each port (on the x axis), the loads compatible with the port's draft limit are depicted with a circle. The y axis reports the load of the ship. The ship tour is depicted as a path, starting from port 0 with load 3 and returning to port 0 with load 0, where each port is visited exactly once.

A useful relaxation of the problem is obtained by removing (14) from F2. In this case, a feasible solution to (15)–(18) is also a tour starting at the port 0 with load Q and ending at the same port with load 0, respecting the draft limits. Nevertheless, such tour does not have to visit all ports, while other ports may be visited more than once. Optimizing this relaxation can be done in $O(n^2Q)$ time by a dynamic programming procedure, which suggests the following reformulation of F2. Let P be a set of all paths defined above. For each $p\in P$, we introduce the binary variable λ_p indicating if p is used or not in the solution. Define q_{ij}^{kp} as a binary coefficient indicating whether variable z_{ij}^k is associated to path p.

$$\min \sum_{p\in P}\left(\sum_{i\in V}\sum_{\substack{j\in V\\ j\neq i}}\sum_{k=d_j}^{K_{ij}} q_{ij}^{kp} c_{ij}\right)\lambda_p \tag{23}$$

$$\text{s.t.} \sum_{p\in P}\left(\sum_{\substack{j\in V\\ j\neq i}}\sum_{k=d_j}^{K_{ij}} q_{ij}^{kp}\right)\lambda_p = 1, \quad \forall i\in V' \tag{24}$$

$$\lambda_p \in \{0,1\} \quad \forall p\in P. \tag{25}$$

An additional constraint r over the z_{ij}^k variables having the format

$$\sum_{i\in V'}\sum_{\substack{j\in V'\\ j\neq i}}\sum_{k=d_i}^{l_i} \alpha_{ij}^{kr} z_{ij}^k \geqslant b_r \tag{26}$$

can be included in F3 as:

$$\sum_{p\in P}\left(\sum_{i\in V'}\sum_{\substack{j\in V'\\ j\neq i}}\sum_{k=d_i}^{l_i} \alpha_{ij}^{kr}\right)\lambda_p \geqslant b_r. \tag{27}$$

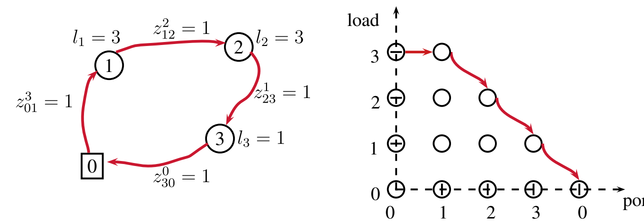

Fig. 1. Path representation of a F2 solution.

The linear relaxation of F3, even with additional cuts, can be solved by column generation. Suppose that, at a given instant, the Master LP has R additional cuts, the r-th cut has dual variable β_r. Constraints (24) have dual variables π. We define the *reduced cost* of the variable $z_{i,j}^k$ as:

$$\bar{c}_{ij}^k = c_{ij} - \pi_i - \sum_{r=1}^{R} \alpha_{ij}^{kr}\beta_r, \tag{28}$$

where $\pi_0 = 0$. The *reduced cost* of a *Master LP* variable λ_p is given by:

$$\bar{\lambda}_p = \sum_{i\in V}\sum_{\substack{j\in V\\ j\neq i}}\sum_{k=d_j}^{K_{ij}} q_{ij}^{kp}\bar{c}_{ij}^k. \tag{29}$$

Therefore, the pricing subproblem can be solved by a shortest path subproblem over the acyclic graph illustrated in Fig. 1, where the arc costs correspond to $\bar{c}_{ij}^k$. This amounts to a shortest path problem with resource constraints over the original graph G.

Significantly stronger linear relaxations can be obtained by forbidding some paths in P that visit some ports more than once. For example, one could avoid tours with s-cycles (Irnich & Villeneuve, 2006), i.e., returning to a port i before visiting at least s ports other than i.

Instead, we use the following strategy that already proved being more efficient in practice (Baldacci et al., 2011). For each customer $i\in V'$, let $N_i \subseteq V'$ be the *ng*-set of i, defining its neighborhood. This may stand for the $|N_i|$ closest ports and includes i itself. The cardinalities of all *ng*-sets are the same, denoted by T. An *ng*-path is a path as defined in P where every cycle that starts and ends at a vertex i must contain at least one vertex j such that $i \notin N_j$. This can be interpreted as if the ship "forgot" the visit to i when passing by the port j. The modified shortest path problem that consider the *ng*-restrictions has a complexity of $O(n^2Q2^T)$. This means that T cannot be very large.

In our implementation, we define a different *ng*-set N_i^k for each load k of the ship after visiting each port i. The neighbors of port i with load k are then selected as the T closest ports that can be visited immediately before i without violating the draft limits and still preserving the same computational complexity. This modification strengthens the relaxation since original *ng*-sets spend part of its memory to store visits to ports that would violate the draft limits. The same pricing algorithm can be used to handle these *ng*-sets. To the best of our knowledge, this is the first time that *ng*-sets depending on the load are considered.

Formulation F3 is then defined as (23)–(27), where P is defined as the set of *ng*-paths, plus all inequalities described in Abeledo et al. (2013) translated to the λ_p variables as shown in (26) and (27). F1 and F2 have a number of variables that is pseudo-polynomial in Q and this may undermine the performance of the resulting algorithms when ports have large demands. These formulations are therefore more suitable when the ports' demands are not very large. The size of formulation F3 does not depend on Q, but the complexity of the column generation subproblem is linearly dependent on Q. Nevertheless, previous studies showed that reasonably large demands can still be handled in practice (Pessoa et al., 2008; Subramanian, Uchoa, Pessoa, & Ochi, 2013). In particular, Pessoa, Uchoa, Poggi, and Rodrigues (2010) solved a multi-machine scheduling problem using an extended formulation. Each job was associated to a processing time up to 100 units and the resulting subproblem would count up to thousands of units of processing time, without compromising the algorithm's computing time.

3. Algorithm description

The branch-and-cut algorithms for formulations F1 and F2 have been implemented using the Callable Libraries of CPLEX, and, the subtour elimination constraints (12) and (21) have been separated using the CVRPSEP Library (Lysgaard, 2003). The subtour constraints have been separated only up to the seventh level of the branching tree to speed up computation. Moreover, at most 50 subtour cuts have been added per iteration. The 2-cycle inequalities (22) were separated only at the root node. CPLEX strong branching was chosen for branching and all CPLEX cuts have been used for strengthening the formulation.

The branch-cut-and-price algorithm for formulation F3 is an adaptation of the one proposed by Abeledo et al. (2013). We enhance it by replacing the 5-cycle elimination in the pricing problem with the *ng*-sets described above with $T = 12$. Preliminary experiments showed that $T = 12$ provides a good compromise: high quality lower bounds are obtained and the computing times remain relatively small. The method starts by only considering Constraints (24) and iteratively adds the remaining inequalities on demand using the separation procedures described by Abeledo et al. (2013). Furthermore, we branch over the x_{ij} variables translated from the z_{ij}^k variables using

$$x_{ij} = \sum_{k=d_j}^{K_{ij}} z_{ij}^k.$$

Given a relaxed solution $\bar{x}$, we choose a pair of ports (i,j) such that $\bar{x}_{ij} + \bar{x}_{ji}$ is strictly between 0 and 1 and add the constraint $x_{ij} + x_{ji} \leqslant 0$ in one branch and $x_{ij} + x_{ji} \geqslant 1$ in the other. These cuts are translated back to the z_{ij}^k variables and then to the λ_p variables. In the selection of the best pair (i,j), we try to maximize the absolute difference between $\bar{x}_{ij} + \bar{x}_{ji}$ and a target value 0.6 by choosing the pair that maximizes

$$\min\{(\bar{x}_{ij} + \bar{x}_{ji})/0.6, (1.0 - \bar{x}_{ij} - \bar{x}_{ji})/0.4\}.$$

4. Computational results

The instances considered in our extensive computational testing belong to the benchmark set proposed by Rakke et al. (2012). The problems are adaptations of instances from the TSPLIB (namely *burma14*, *ulysees16*, *ulysses22*, *fri26*, *bayg29*, *gr17*, *gr21*, and *gr48*), with number of vertices ranging between 14 and 48. In the following, the acronym *a_b_c* refers to the c^{th} instance, adapted from the TSPLIB problem *a* with *b*% of ports with draft limit smaller than Q.

For each TSP instance, problems with 10%, 25% and 50% of the ports having a draft limit smaller than Q have been generated and each port has unitary demand. More precisely, given each TSP instance and each percentage of ports with drafts smaller than Q, ten instances were proposed. Drafts smaller than Q were randomly generated between 1 and $n-1$. The instances are available at http://jgr.no/tspdl.

Our tests were performed on an Intel Core i5 with 3.2 gigahertz and 4 gigabyte of RAM, running Ubuntu Linux 10.04. A two-hours time limit was imposed and a single thread used throughout the computational experience.

In the following, we compare the root node lower bounds of F1, F2, and F3 (including or not additional constraints). Detailed results can be found in the Appendix (Tables B.3–B.8). For each *Instance* and each formulation, the percentage deviation of lower bound z with respect to the optimal solution z_{opt} is computed as:

$$Dev(\%) = 100 \times \left(1 - \frac{z}{z_{opt}}\right).$$

A summary of our results is provided in Table 1, where for each set of instances the average percentage deviation from the optimal solutions ($Dev(\%)$) and average computing time in seconds (*Time*(*seconds*)) are provided. The average geometric deviation is also reported and computed for each set of instances I as:

$$G.Dev(\%) = 100 \times \left(1 - \sqrt[|I|]{\frac{z_1}{z_{opt1}} \times \cdots \times \frac{z_{|I|}}{z_{opt|I|}}}\right).$$

The average computing times in seconds are reported in the columns *Time*(*seconds*).

Both F1 and F2 dramatically improve their performance when subtour elimination constraints are adopted. F1 with Constraints (12) reduces the average optimality gap with respect to F1 by almost 5%, whereas F2 with Constraints (21) by 1.5%. The average gap of formulation F1 is high (10.68%, and 14.65% for the *gr*48 instances), whereas F2 produces better quality lower bounds (the average gap is 4.53%). F2 is also roughly five times faster than F1.

Table 1
Root node lower bounds: summary of the average results.

Instance	F1			F1 + (12)			F2			F2 + (21)			F2 + (21) + (22)			F3		
	Dev. (%)	G.Dev. (%)	Time (seconds)	Dev. (%)	G.Dev. (%)	Time (seconds)	Dev. (%)	G.Dev. (%)	Time (seconds)	Dev. (%)	G.Dev. (%)	Time (seconds)	Dev. (%)	G.Dev. (%)	Time (seconds)	Dev. (%)	G.Dev. (%)	Time (seconds)
burma14	6.54	6.63	0.46	2.57	2.65	0.44	0.49	0.50	0.27	0.39	0.39	0.23	0.16	0.44	0.19	0.00	0.00	0.38
ulysses16	6.82	6.92	0.84	1.52	1.56	0.72	0.55	0.56	0.48	0.36	0.37	0.33	0.2	0.36	0.34	0.00	0.00	24.45
ulysses22	12.13	12.24	3.24	5.5	5.66	4.26	6.05	6.14	2	3.69	3.79	1.95	2.56	3.45	2.49	0.00	0.00	27.73
fri26	12.33	12.52	6.96	7.9	8.07	8.59	6.59	6.63	4.04	3.95	3.99	4.29	2.34	4.18	6.79	0.00	0.00	15.02
bayg29	10.23	10.40	14.86	7.13	7.32	18.99	6.37	6.41	6.22	4.11	4.16	6.74	2.65	4.13	13.38	0.00	0.00	12.14
gr17	15.02	15.15	1.08	2.9	2.98	0.98	2.58	2.61	0.65	0.34	0.35	0.42	0.22	0.65	0.41	0.00	0.00	13.92
gr21	7.72	7.96	2.18	7.37	7.59	2.29	4.1	4.18	0.95	3.96	4.03	1.03	2.05	3.81	1.22	0.00	0.00	11.13
gr48	14.65	14.93	375.63	11.24	11.55	606.14	9.51	9.57	76.79	7.2	7.27	109.27	5.05	7.27	274.72	0.84	0.85	125.22
Avg.	10.68	10.90	50.66	5.77	5.98	80.30	4.53	4.62	11.42	3.00	3.07	15.53	1.90	3.06	37.44	0.11	0.11	28.75

Table 2
Optimal solutions: summary of the number of optimal solutions achieved.

	Rakke et al. (2012)	F1 + (12)	F1 + (12) + CPLEX CUTS	F2 + (21) + (22)	F2 + (21) + (22) + CPLEX CUTS	F3
burma14	30	30	30	30	30	30
ulysses16	30	30	30	30	30	30
ulysses22	27	25	17	30	30	30
fri26	23	23	13	30	30	30
bayg29	19	17	14	30	30	30
gr17	30	30	30	30	30	30
gr22	30	30	26	30	30	30
gr48	7	0	1	4	4	30
Total	196	185	161	214	214	240

Constraints (22) reduce substantially the optimality gap and roughly double the average computing time.

F3 provides highly competitive bounds: all instances, except some of the *gr*48 instances, have been solved to optimality at the root node, in less than roughly 30 seconds on average. The average computing times are almost doubled with respect to F2 with Constraints (21), but the average overall deviation is much smaller (3% for F2 with subtour constraints and 0.11% for F3).

In terms of optimal solutions achieved, we compare the best bounds provided by Rakke et al. (2012) with those obtained by F1 with (12), F2 with (21) and (22) and F3. The experiments conducted by Rakke et al. (2012) had been performed on a HP dl160 G3 computer with 2×3.0 gigahertz Intel E5472 Xeon CPU and 16 gigabyte of RAM. The solver used was Xpress-MP 7.2 and the separation routine for the subtour elimination constraints was coded in C++ using the Mosel 3.2.0 callbacks. Finally, the algorithm was executed using parallel processing on the 8 cores available on the machine and for at most 10,000 seconds. Our testing has been performed on a more modest computer, using a single core and a 7200 seconds time limit, therefore our results are not directly comparable to those of Rakke et al. (2012).

The upper and lower bounds achieved by the best branch-and-cut of Rakke et al. (2012), the branch-and-cuts of F1 with (12) and of F2 with (21) and (22), and the branch-cut-and-price F3 are given in Tables C.9–C.14, as well as the computing times and the number of nodes explored are provided. The bold-faced values are the non-optimal solution values. Note that the implementations of F1 and F2 benefit from the CPLEX cuts, whereas F3 does not make use of these inequalities.

A summary of these results can be found in Table 2, where the number of optimal solutions achieved for each benchmark set is given. Table 2 presents also results for F1 and F2 without considering CPLEX cuts: this allows for a more comprehensive comparison with the results of Rakke et al. (2012), where these cuts are not implemented.

Even if the number of optimal solutions obtained by Rakke et al. (2012) is higher than that of F1, it is interesting to observe that F1 is not dominated. Example of problems in which F1 outperforms Rakke et al. (2012) algorithms with or without CPLEX cuts are available, even if F1 is executed on a slower computer and for a shorter amount of time. F1 performs remarkably better without CPLEX cuts when small instances are considered, but the CPLEX cuts allow for solving to optimality one of the *gr*48 instances. F2 is capable of solving 214 out of the 240 instances in the set, but only 4 of the *gr*48 instances. CPLEX cuts do not affect the number of optimal solutions obtained by F2. F3 solves to optimality all instances in the set.

5. Conclusions

In this paper, we presented three exact algorithms for the TSPDL. The first algorithm is a branch-and-cut and it is based on a compact formulation in which two sets of two-index binary variables and a polynomial number of constraints are employed. This formulation, when strengthened with subtour elimination constraints and trivial constraints is not empirically dominated by the best formulation proposed by Rakke et al. (2012). The second algorithm is also a branch-and-cut, but the underlying formulation considers three index variables. This formulation is proven to dominate the first one, both theoretically and empirically. The third algorithm is a branch-cut-and-price and it is based on a Dantzig–Wolfe decomposition of the second formulation. Columns are generated by dynamically introducing *ng*-paths to the formulation. The latter algorithm was capable of solving to optimality all the benchmark instances from the literature.

Acknowledgements

The authors would like to thank Prof. Marielle Christiansen and Dr. Jørgen Glomvik Rakke for providing their results. This work was partially supported by Santander Universities UK, UoS Internationalisation Fund, by CORMSIS, Centre of Operational Research, Management Sciences and Information Systems, and Brazilian research agencies CNPq, CAPES and FAPERJ.

Appendix A. Proof: F2 dominates F1

Proof. A $\overline{z_{ij}^k}$ solution of F2 can be converted into an F1 solution $(\overline{x_{ij}}, \overline{y_{jk}})$ with the same cost, considering the following transformation:

$$\begin{cases} \overline{x_{ij}} = \sum_{k=d_j}^{K_{ij}} \overline{z_{ij}^k} & \forall (i,j) \in A \\ \overline{y_{ik}} = \sum_{\substack{s \in V | s \neq i \\ l_s \geqslant k+d_s}} \overline{z_{si}^k}, & \forall i \in V', \quad k = \{d_i, \ldots, l_i\} \end{cases}$$

It is straightforward that, given $(\overline{x_{ij}}, \overline{y_{jp}})$, Constraints (2), (3) and (5) are implied by constraints in F2. In fact, once converted into $\overline{z_{ij}^k}$ variables, they correspond to Constraints (14), (19), and (14), respectively. According to Constraints (17), Q units of load are shipped from the origin port and, from Constraints (16), zero units return to the same port. Moreover, Constraints (15) guarantee that the load monotonically decreases in the tour defined by Constraints (14) and (15). Hence, Constraints (4), (6) and (7) are satisfied by F2. In the following we prove that Constraints (8) are satisfied by F2: we first express the constraints in term of z_{ij}^k variables

$$x_{ij} + y_{ik} = \sum_{p=d_j}^{K_{ij}} z_{ij}^p + \sum_{\substack{s \in V | s \neq i \\ l_s \geqslant k+d_s}} z_{si}^k.$$

Given Constraints (15), we can write:

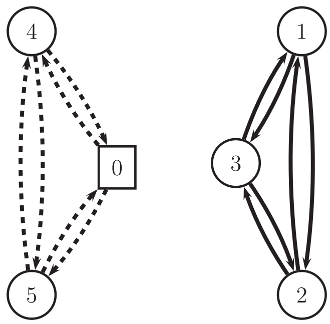

Fig. A.2. Fractional solution of F1 presenting subtours.

$$\sum_{p=d_j}^{K_{ij}} z_{ij}^p + \sum_{\substack{s\in V|s\neq i\\ l_s\geqslant k+d_s}} z_{si}^k = \sum_{p=d_j}^{K_{ij}} z_{ij}^p + \sum_{\substack{s\in V|s\neq i\\ l_s\geqslant k-d_i, d_s\leqslant k-d_i}} z_{is}^{k-d_i}$$

The latter term can be overestimated by

$$\sum_{p=d_j}^{K_{ij}} z_{ij}^p + \sum_{\substack{s\in V|s\neq i\\ l_s\geqslant k-d_i, d_s\leqslant k-d_i}} z_{is}^{k-d_i} \leqslant \sum_{s\in V, s\neq i} \sum_{p=d_s}^{K_{is}} z_{is}^p + z_{ij}^{k-d_i}.$$

Given Constraints (19)

$$\sum_{s\in V, s\neq i} \sum_{p=d_s}^{K_{is}} z_{is}^p + z_{ij}^{k-d_i} = 1 + z_{ij}^{k-d_i}.$$

This can be overestimated by

$$1 + z_{ij}^{k-d_i} \leqslant 1 + \sum_{\substack{s\in V|s\neq j\\ l_s\geqslant k-d_i+d_s}} z_{sj}^{k-d_i} = 1 + y_{j,k-d_i}.$$

Therefore, Constraints (8) are satisfied.

The linear relaxation of F1 allows for disconnected subtours with at least three vertices of lower cost than the corresponding integer connected solution, as the ones depicted in Fig. A.2. Such fractional solutions are not feasible for F2, because Constraints (15) ensure connectivity. Therefore the feasible region of the linear relaxation of F2 is a subset of the feasible region of the linear relaxation of F1. □

Appendix B. Root node results

See Tables B.3–B.8.

Appendix C. Best bounds

See Tables C.9–C.14.

Table B.3
Root node lower bounds: *burma* instances.

Instance	F1		F1 + (12)		F2		F2 + (21)		F2 + (21) + (22)		F3	
	Dev. (%)	Time (seconds)	Dev. (%)	Time (seconds)	Dev. (%)	Time (seconds)	Dev. (%)	Time (seconds)	Dev. (%)	Time (seconds)	Dev. (%)	Time (seconds)
burma14_10_1	1.79	0.44	0.00	0.08	0.03	0.13	0.00	0.12	0.00	0.13	0.00	0.34
burma14_10_2	6.77	0.37	0.00	0.17	0.00	0.34	0.00	0.19	0.00	0.19	0.00	0.68
burma14_10_3	6.77	0.36	0.00	0.15	0.00	0.13	0.00	0.13	0.00	0.13	0.00	0.39
burma14_10_4	3.79	0.56	1.61	0.46	1.19	0.59	0.00	0.36	0.00	0.31	0.00	0.58
burma14_10_5	5.82	0.43	0.00	0.15	0.00	0.40	0.00	0.16	0.00	0.15	0.00	0.37
burma14_10_6	6.77	0.49	0.00	0.23	0.00	0.24	0.00	0.13	0.00	0.13	0.00	0.63
burma14_10_7	5.80	0.36	0.00	0.15	0.00	0.53	0.00	0.15	0.00	0.16	0.00	0.44
burma14_10_8	7.41	0.31	0.00	0.34	0.00	0.20	0.00	0.11	0.00	0.12	0.00	0.33
burma14_10_9	8.34	0.39	1.18	0.89	0.00	0.43	0.00	0.23	0.00	0.23	0.00	0.40
burma14_10_10	6.77	0.43	0.00	0.29	0.00	0.34	0.00	0.15	0.00	0.16	0.00	0.62
burma14_25_1	16.42	0.82	14.34	0.97	0.00	0.32	0.00	0.32	0.00	0.18	0.00	0.32
burma14_25_2	7.47	0.40	2.98	0.80	0.00	0.40	0.00	0.48	0.00	0.21	0.00	0.34
burma14_25_3	0.00	0.06	0.00	0.06	0.00	0.03	0.00	0.03	0.00	0.03	0.00	0.29
burma14_25_4	11.69	0.78	5.59	0.89	3.08	0.44	2.46	0.46	1.55	0.50	0.00	0.31
burma14_25_5	7.41	0.33	0.69	0.46	0.00	0.27	0.30	0.21	0.00	0.14	0.00	0.45
burma14_25_6	0.32	0.33	0.00	0.11	0.00	0.10	0.00	0.10	0.00	0.10	0.00	0.30
burma14_25_7	7.41	0.34	0.00	0.38	0.00	0.17	0.00	0.15	0.00	0.15	0.00	0.35
burma14_25_8	6.42	0.42	0.91	0.28	0.00	0.44	0.00	0.23	0.00	0.24	0.00	0.41
burma14_25_9	15.02	0.94	11.01	0.82	0.00	0.28	0.00	0.56	0.00	0.31	0.00	0.36
burma14_25_10	10.82	0.85	8.91	0.82	0.00	0.39	1.22	0.44	0.00	0.39	0.00	0.31
burma14_50_1	9.19	0.62	8.74	0.87	4.32	0.23	4.91	0.22	3.21	0.23	0.00	0.30
burma14_50_2	0.00	0.59	0.00	0.27	0.00	0.17	0.00	0.18	0.00	0.18	0.00	0.30
burma14_50_3	0.00	0.08	0.00	0.09	0.00	0.06	0.00	0.07	0.00	0.07	0.00	0.30
burma14_50_4	4.38	0.36	0.00	0.15	0.00	0.05	0.00	0.06	0.00	0.05	0.00	0.29
burma14_50_5	0.00	0.15	0.00	0.14	0.00	0.08	0.00	0.08	0.00	0.08	0.00	0.39
burma14_50_6	4.88	0.32	1.77	0.49	1.83	0.30	1.49	0.19	0.00	0.15	0.00	0.28
burma14_50_7	7.72	0.38	1.76	0.58	4.27	0.26	1.24	0.45	0.00	0.23	0.00	0.34
burma14_50_8	5.47	0.73	3.37	0.35	0.00	0.18	0.00	0.18	0.00	0.18	0.00	0.35
burma14_50_9	9.61	0.67	4.73	0.71	0.00	0.22	0.00	0.34	0.00	0.25	0.00	0.31
burma14_50_10	11.91	0.56	9.49	1.08	0.00	0.34	0.00	0.29	0.00	0.23	0.00	0.30

Table B.4
Root node lower bounds: *ulysses* instances.

Instance	F1		F1 + (12)		F2		F2 + (21)		F2 + (21) + (22)		F3	
	Dev. (%)	Time (seconds)	Dev. (%)	Time (seconds)	Dev. (%)	Time (seconds)	Dev. (%)	Time (seconds)	Dev. (%)	Time (seconds)	Dev. (%)	Time (seconds)
ulysses16_10_1	10.54	0.63	0.00	0.46	0.00	0.48	0.00	0.21	0.00	0.20	0.00	33.70
ulysses16_10_2	9.03	1.07	0.00	0.49	0.00	0.46	0.00	0.22	0.00	0.24	0.00	46.58
ulysses16_10_3	10.54	0.55	0.00	0.29	1.94	0.79	0.00	0.23	0.00	0.25	0.00	72.22
ulysses16_10_4	6.14	1.63	0.00	0.38	0.00	0.58	0.00	0.23	0.00	0.21	0.00	32.90
ulysses16_10_5	10.54	0.77	0.00	0.31	0.00	0.51	0.00	0.21	0.00	0.23	0.00	59.85
ulysses16_10_6	9.39	1.03	0.92	0.61	0.00	0.38	0.00	0.37	0.00	0.38	0.00	32.43
ulysses16_10_7	10.54	0.73	0.00	0.45	0.22	0.63	0.00	0.24	0.00	0.33	0.00	62.17
ulysses16_10_8	10.54	0.65	0.00	0.49	0.28	0.58	0.00	0.20	0.00	0.21	0.00	40.47
ulysses16_10_9	8.92	0.95	0.00	0.44	0.00	0.57	0.00	0.30	0.00	0.34	0.00	74.81
ulysses16_10_10	10.54	0.70	0.00	0.49	1.66	0.57	0.00	0.27	0.00	0.28	0.00	48.29
ulysses16_25_1	9.51	0.73	0.40	1.06	0.00	0.70	0.00	0.57	0.00	0.56	0.00	49.34
ulysses16_25_2	1.46	0.46	0.00	0.29	0.00	0.46	0.00	0.31	0.00	0.32	0.00	3.93
ulysses16_25_3	1.18	0.89	0.00	0.25	0.42	0.85	0.00	0.37	0.00	0.37	0.00	21.82
ulysses16_25_4	1.58	1.19	1.10	1.42	0.00	0.44	0.00	0.52	0.00	0.42	0.00	3.48
ulysses16_25_5	11.57	0.93	9.14	1.52	0.00	0.63	0.00	0.61	0.00	0.48	0.00	11.04
ulysses16_25_6	5.11	0.99	0.00	0.60	0.00	0.23	0.00	0.36	0.00	0.31	0.00	10.07
ulysses16_25_7	4.00	0.99	2.51	1.09	0.00	0.76	0.00	0.69	0.00	0.70	0.00	9.75
ulysses16_25_8	10.54	0.50	0.00	0.72	1.11	0.85	0.00	0.24	0.00	0.27	0.00	42.86
ulysses16_25_9	1.15	0.73	0.00	0.25	0.00	0.15	0.00	0.14	0.00	0.15	0.00	11.25
ulysses16_25_10	11.61	1.15	9.88	1.70	5.23	0.97	6.08	0.68	3.24	1.10	0.00	21.14
ulysses16_50_1	3.59	0.92	2.82	1.05	0.62	0.56	0.00	0.44	0.00	0.47	0.00	2.02
ulysses16_50_2	4.58	0.76	1.77	0.85	0.00	0.26	0.00	0.27	0.00	0.27	0.00	2.53
ulysses16_50_3	1.58	0.36	0.00	0.25	0.00	0.08	0.00	0.08	0.00	0.08	0.00	1.16
ulysses16_50_4	3.42	1.45	3.36	0.92	0.00	0.28	0.00	0.28	0.00	0.31	0.00	1.19
ulysses16_50_5	2.87	0.60	0.00	0.82	0.00	0.32	0.00	0.19	0.00	0.19	0.00	9.85
ulysses16_50_6	7.58	1.29	1.30	1.00	0.00	0.22	0.00	0.28	0.00	0.24	0.00	3.61
ulysses16_50_7	15.31	0.82	10.90	1.46	5.02	0.52	4.83	0.68	2.63	0.56	0.00	3.01
ulysses16_50_8	0.00	0.19	0.00	0.09	0.00	0.05	0.00	0.05	0.00	0.05	0.00	2.36
ulysses16_50_9	9.64	0.55	0.06	1.04	0.00	0.34	0.00	0.32	0.00	0.27	0.00	11.73
ulysses16_50_10	1.69	0.97	1.32	0.92	0.00	0.19	0.00	0.31	0.00	0.29	0.00	7.87
ulysses22_10_1	9.45	3.13	0.00	4.65	1.76	2.57	0.00	0.96	0.00	0.96	0.00	35.45
ulysses22_10_2	9.35	3.08	0.00	1.63	3.91	2.75	0.00	0.93	0.00	0.82	0.00	26.35
ulysses22_10_3	9.45	3.74	0.00	1.15	6.50	2.09	0.00	0.54	0.00	0.56	0.00	27.92
ulysses22_10_4	9.45	2.72	0.00	4.68	6.28	1.70	0.00	1.04	0.00	0.81	0.00	19.65
ulysses22_10_5	8.76	3.27	0.00	1.10	0.00	1.87	0.00	1.08	0.00	1.20	0.00	38.99
ulysses22_10_6	8.76	2.38	0.63	6.87	2.46	1.64	0.00	1.02	0.00	1.10	0.00	40.32
ulysses22_10_7	12.37	2.42	3.22	4.58	8.64	1.65	2.98	2.26	2.25	3.96	0.00	40.00
ulysses22_10_8	11.07	2.88	1.99	4.56	0.00	1.53	0.00	1.19	0.00	1.23	0.00	55.60
ulysses22_10_9	4.29	4.11	0.00	1.06	2.84	1.92	0.00	0.91	0.00	0.97	0.00	18.12
ulysses22_10_10	10.40	3.11	1.00	6.70	6.50	2.31	0.74	3.09	0.26	4.05	0.00	17.79
ulysses22_25_1	9.99	3.62	0.86	6.98	2.56	2.47	0.71	1.52	0.65	2.86	0.00	30.45
ulysses22_25_2	14.36	3.50	5.14	3.96	8.64	1.72	4.53	3.37	3.23	3.87	0.00	19.15
ulysses22_25_3	8.31	2.94	7.01	3.79	7.96	1.63	6.74	1.49	6.10	1.74	0.00	21.84
ulysses22_25_4	13.97	3.09	4.59	5.78	8.72	2.02	4.35	2.55	2.50	5.83	0.00	28.55
ulysses22_25_5	13.84	2.90	5.47	6.10	4.57	2.61	2.27	3.78	1.69	5.28	0.00	23.40
ulysses22_25_6	16.20	3.04	7.30	4.88	7.59	2.16	5.51	1.81	3.07	3.91	0.00	32.14
ulysses22_25_7	16.61	3.20	9.05	6.55	11.00	2.01	7.71	2.51	5.96	3.99	0.00	23.71
ulysses22_25_8	8.24	4.09	1.50	5.16	3.72	1.70	1.04	2.47	0.00	1.25	0.00	17.34
ulysses22_25_9	8.93	3.35	0.00	4.28	2.24	2.63	0.00	2.44	0.00	1.71	0.00	26.91
ulysses22_25_10	1.09	3.62	0.00	2.16	0.00	1.75	0.00	1.05	0.00	1.07	0.00	22.62
ulysses22_50_1	11.31	3.25	9.79	4.36	9.64	1.44	7.47	1.59	5.78	3.55	0.00	24.07
ulysses22_50_2	15.71	2.22	6.36	4.51	9.36	2.46	5.14	3.10	3.18	3.77	0.00	16.47
ulysses22_50_3	19.52	3.80	17.45	4.13	19.00	1.51	19.00	1.53	19.00	1.95	0.00	21.56
ulysses22_50_4	18.35	3.13	17.62	4.64	1.88	1.64	4.34	2.21	0.00	2.24	0.00	38.34
ulysses22_50_5	13.65	4.71	10.91	4.16	3.40	2.67	2.10	3.03	2.41	2.16	0.00	45.84
ulysses22_50_6	15.79	3.48	6.77	4.07	5.88	2.01	4.27	2.44	0.00	2.90	0.00	10.52
ulysses22_50_7	19.59	2.63	11.09	4.79	3.80	2.20	3.25	3.21	0.00	1.68	0.00	25.26
ulysses22_50_8	10.64	4.02	11.06	3.64	8.71	1.77	7.41	1.85	6.00	2.17	0.00	20.55
ulysses22_50_9	19.87	2.36	14.96	2.93	11.35	1.60	10.83	1.43	8.34	2.67	0.00	47.84
ulysses22_50_10	14.49	3.53	11.09	3.85	12.47	2.09	10.27	2.03	6.50	4.41	0.00	15.06

Table B.5
Root node lower bounds: *fri* instances.

Instance	F1		F1 + (12)		F2		F2 + (21)		F2 + (21) + (22)		F3	
	Dev. (%)	Time (seconds)	Dev. (%)	Time (seconds)	Dev. (%)	Time (seconds)	Dev. (%)	Time (seconds)	Dev. (%)	Time (seconds)	Dev. (%)	Time (seconds)
fri26_10_1	5.34	9.64	0.00	3.42	4.34	4.34	0.00	1.44	0.00	1.68	0.00	11.88
fri26_10_2	5.76	8.16	0.00	3.77	4.32	2.80	0.00	1.68	0.00	1.72	0.00	11.23
fri26_10_3	11.93	7.08	7.08	11.94	6.13	6.21	3.88	5.80	2.01	9.23	0.00	14.42
fri26_10_4	6.89	8.74	1.85	7.81	5.43	3.74	1.82	2.16	1.52	3.81	0.00	12.51
fri26_10_5	11.43	5.87	6.02	6.98	6.91	4.43	1.85	6.48	0.00	9.40	0.00	21.78
fri26_10_6	5.60	6.77	0.00	4.57	4.27	3.57	0.00	1.17	0.00	1.29	0.00	8.46
fri26_10_7	15.01	5.99	9.82	9.05	11.33	4.87	7.65	6.14	5.85	9.79	0.00	14.14
fri26_10_8	7.35	7.62	0.97	13.62	5.38	3.67	1.06	5.73	0.00	5.88	0.00	8.27
fri26_10_9	3.40	7.09	0.00	2.31	2.59	3.78	0.00	2.03	0.00	2.05	0.00	11.12
fri26_10_10	5.76	6.57	0.00	3.71	4.41	3.37	0.00	1.43	0.00	1.88	0.00	9.87
fri26_25_1	12.54	6.64	7.46	9.78	7.48	3.33	4.31	4.85	2.00	7.98	0.00	14.60
fri26_25_2	11.42	8.47	10.32	7.81	4.78	4.68	4.28	4.23	2.48	10.86	0.00	26.75
fri26_25_3	9.62	7.21	9.53	10.88	4.68	4.37	2.99	5.04	2.37	5.60	0.00	24.18
fri26_25_4	26.03	9.86	20.47	13.60	7.30	4.57	8.20	4.89	6.44	8.38	0.00	24.63
fri26_25_5	11.54	7.99	7.50	12.89	10.15	4.37	6.79	3.93	4.70	10.18	0.00	14.87
fri26_25_6	22.15	5.11	16.83	11.31	9.27	4.11	5.96	8.34	3.63	9.69	0.00	14.68
fri26_25_7	19.80	5.79	14.90	6.00	10.90	5.53	7.31	8.17	3.66	10.55	0.00	18.88
fri26_25_8	7.02	6.94	1.81	12.47	5.14	4.10	1.74	3.85	1.10	5.89	0.00	6.39
fri26_25_9	17.11	5.74	11.83	12.58	10.42	5.44	8.27	6.24	5.08	14.34	0.00	10.16
fri26_25_10	11.13	6.29	5.01	10.78	9.07	2.57	5.08	3.71	4.13	10.31	0.00	9.13
fri26_50_1	24.75	5.73	18.97	8.57	5.00	4.11	6.77	3.46	2.45	7.84	0.00	16.54
fri26_50_2	13.43	6.21	9.81	7.59	10.39	3.97	6.81	4.84	5.33	9.35	0.00	22.10
fri26_50_3	11.57	5.53	7.10	7.59	7.39	4.87	4.84	5.80	2.77	10.01	0.00	12.46
fri26_50_4	11.64	6.68	11.16	7.50	4.17	4.32	4.23	3.92	1.99	5.42	0.00	12.04
fri26_50_5	16.47	4.92	11.79	7.62	4.26	2.68	2.09	4.18	0.00	2.29	0.00	12.50
fri26_50_6	14.56	4.15	8.01	8.19	4.42	3.39	3.22	3.71	1.76	4.96	0.00	9.84
fri26_50_7	15.35	6.76	8.97	10.58	2.93	5.60	1.93	5.63	0.00	5.86	0.00	14.63
fri26_50_8	10.18	6.97	6.42	9.11	6.08	1.81	4.44	2.71	2.10	2.10	0.00	22.23
fri26_50_9	10.84	11.41	13.94	6.79	6.66	3.30	6.63	2.80	3.86	6.92	0.00	28.37
fri26_50_10	14.41	6.71	9.39	8.98	12.20	3.27	6.39	4.40	5.08	8.39	0.00	11.89

Table B.6
Root node lower bounds: *bayg* instances.

Instance	F1		F1 + (12)		F2		F2 + (21)		F2 + (21) + (22)		F3	
	Dev. (%)	Time (seconds)	Dev. (%)	Time (seconds)	Dev. (%)	Time (seconds)	Dev. (%)	Time (seconds)	Dev. (%)	Time (seconds)	Dev. (%)	Time (seconds)
bayg29_10_1	3.85	21.96	0.00	18.00	3.51	4.89	0.00	5.36	0.00	4.88	0.00	10.88
bayg29_10_2	6.41	10.12	2.66	17.09	5.63	5.72	2.41	7.45	1.43	18.63	0.00	9.81
bayg29_10_3	11.22	15.41	6.83	27.02	3.57	6.67	1.42	4.49	0.93	11.48	0.00	11.66
bayg29_10_4	3.52	22.50	0.27	32.14	0.75	6.73	0.00	4.02	0.00	3.41	0.00	8.26
bayg29_10_5	5.89	20.99	2.13	16.59	4.94	6.61	2.03	4.94	1.36	14.10	0.00	12.51
bayg29_10_6	4.56	16.10	0.74	34.82	4.19	7.26	0.66	5.94	0.50	12.87	0.00	10.07
bayg29_10_7	7.20	10.87	3.49	17.40	6.31	4.85	2.81	5.35	1.79	15.91	0.00	11.02
bayg29_10_8	3.20	11.96	0.00	3.87	2.78	6.16	0.00	5.97	0.00	5.42	0.00	17.57
bayg29_10_9	4.61	19.76	1.04	30.10	4.44	5.49	1.11	9.49	0.46	16.36	0.00	14.76
bayg29_10_10	6.33	20.88	2.40	50.42	5.88	5.71	2.26	15.22	1.55	25.99	0.00	13.38
bayg29_25_1	14.15	19.99	13.29	16.29	5.58	8.30	3.51	7.27	2.06	10.35	0.00	10.54
bayg29_25_2	6.13	17.02	2.45	34.86	5.62	6.18	2.25	8.88	1.54	14.59	0.00	14.10
bayg29_25_3	14.69	15.11	11.69	14.56	10.53	5.61	5.93	9.59	4.98	44.93	0.00	16.29
bayg29_25_4	13.77	13.12	10.33	15.58	10.48	7.63	8.47	7.62	6.53	17.35	0.00	10.13
bayg29_25_5	8.83	14.85	4.30	18.57	5.50	7.28	2.81	11.27	1.88	19.17	0.00	15.03
bayg29_25_6	4.10	12.08	1.25	21.15	2.90	7.54	0.67	6.82	0.16	10.67	0.00	9.74
bayg29_25_7	13.94	12.88	10.33	21.92	10.62	6.22	7.26	8.09	4.65	16.10	0.00	9.02
bayg29_25_8	9.81	15.90	5.88	24.72	7.52	6.87	4.97	5.53	3.39	13.50	0.00	10.86
bayg29_25_9	7.94	13.26	4.27	19.74	6.71	6.70	4.04	5.35	2.06	14.97	0.00	7.97
bayg29_25_10	2.95	16.55	0.00	4.27	2.74	3.37	0.00	0.67	0.00	0.82	0.00	6.82
bayg29_50_1	17.96	12.04	15.48	13.16	8.56	7.95	7.81	7.23	4.85	12.23	0.00	14.07
bayg29_50_2	16.76	9.35	14.25	11.39	5.10	5.24	4.85	4.74	2.00	12.46	0.00	11.19
bayg29_50_3	17.34	9.58	14.79	12.06	10.67	7.44	8.49	8.61	5.62	13.65	0.00	10.95
bayg29_50_4	17.22	16.12	13.70	18.71	11.62	5.62	10.32	6.13	7.78	10.66	0.00	9.18
bayg29_50_5	9.13	14.94	7.61	13.22	4.70	7.40	2.98	6.33	1.06	13.55	0.00	8.59
bayg29_50_6	13.99	9.08	13.18	9.43	7.28	3.52	7.38	4.24	4.33	9.43	0.00	11.08
bayg29_50_7	14.83	7.86	10.25	13.72	9.51	6.06	6.91	7.17	4.55	14.77	0.00	11.24
bayg29_50_8	24.31	10.63	21.22	11.70	9.74	7.56	10.30	7.27	6.64	7.82	0.00	34.53
bayg29_50_9	15.15	12.87	12.56	11.85	11.38	3.76	9.13	4.27	6.39	9.29	0.00	12.89
bayg29_50_10	7.14	21.92	7.58	15.51	2.25	6.13	2.39	6.98	1.07	5.99	0.00	10.07

Table B.7
Root node lower bounds: *gr* instances, first part.

Instance	F1		F1 + (12)		F2		F2 + (21)		F2 + (21) + (22)		F3	
	Dev. (%)	Time (seconds)	Dev. (%)	Time (seconds)	Dev. (%)	Time (seconds)	Dev. (%)	Time (seconds)	Dev. (%)	Time (seconds)	Dev. (%)	Time (seconds)
gr17_10_1	16.96	1.21	1.77	1.56	0.00	0.30	0.00	0.22	0.00	0.23	0.00	21.74
gr17_10_2	10.45	0.94	0.00	0.33	2.07	0.50	0.00	0.20	0.00	0.21	0.00	28.51
gr17_10_3	17.51	1.32	0.00	0.49	5.91	0.77	0.00	0.31	0.00	0.40	0.00	34.42
gr17_10_4	0.00	0.19	0.00	0.20	0.00	0.29	0.00	0.30	0.00	0.29	0.00	18.25
gr17_10_5	17.51	1.33	0.00	0.54	4.69	0.66	0.00	0.40	0.00	0.36	0.00	23.82
gr17_10_6	17.51	1.09	0.00	0.46	4.55	0.83	0.00	0.25	0.00	0.28	0.00	24.76
gr17_10_7	16.71	1.44	0.00	0.41	3.42	0.92	0.00	0.42	0.00	0.44	0.00	26.18
gr17_10_8	16.87	0.78	0.00	0.40	3.20	1.18	0.00	0.51	0.00	0.51	0.00	2.65
gr17_10_9	17.51	1.04	0.00	1.12	4.06	0.80	0.00	0.38	0.00	0.38	0.00	24.90
gr17_10_10	17.55	1.22	0.00	0.54	5.15	1.10	0.00	0.29	0.00	0.33	0.00	45.95
gr17_25_1	20.83	0.87	6.14	1.33	3.18	0.76	0.83	0.80	0.00	0.51	0.00	3.05
gr17_25_2	22.85	1.39	14.73	1.69	8.64	0.90	5.72	1.02	3.57	1.13	0.00	16.36
gr17_25_3	10.77	0.62	1.32	1.02	2.58	0.68	0.00	0.40	0.00	0.36	0.00	4.23
gr17_25_4	17.99	1.29	0.62	1.46	0.00	0.58	0.00	0.35	0.00	0.31	0.00	19.97
gr17_25_5	17.67	0.75	0.14	1.01	3.86	1.03	0.00	0.40	0.00	0.47	0.00	22.00
gr17_25_6	16.40	1.92	3.40	1.39	2.29	0.52	0.00	0.27	0.00	0.24	0.00	9.22
gr17_25_7	16.98	1.18	0.00	0.55	4.14	0.75	0.00	0.32	0.00	0.34	0.00	15.80
gr17_25_8	16.98	0.88	0.00	0.32	3.79	0.74	0.00	0.21	0.00	0.23	0.00	10.42
gr17_25_9	17.41	0.83	0.00	1.32	2.33	0.78	0.00	0.47	0.00	0.47	0.00	1.90
gr17_25_10	14.54	1.16	9.37	1.76	0.00	0.62	0.00	0.80	0.00	0.76	0.00	8.15
gr17_50_1	14.01	2.16	9.62	2.05	0.00	0.64	0.00	0.59	0.00	0.57	0.00	9.40
gr17_50_2	17.12	1.07	3.15	1.44	0.00	0.31	0.00	0.28	0.00	0.26	0.00	6.61
gr17_50_3	4.86	1.41	5.57	0.87	0.00	0.41	0.00	0.35	0.00	0.35	0.00	1.74
gr17_50_4	11.45	0.90	3.32	1.45	0.61	0.64	0.00	0.44	0.00	0.37	0.00	4.66
gr17_50_5	18.05	1.11	4.82	1.28	6.08	0.75	0.00	0.60	0.00	0.67	0.00	19.25
gr17_50_6	8.06	0.39	0.00	0.25	0.00	0.36	0.00	0.30	0.00	0.30	0.00	2.59
gr17_50_7	13.34	1.43	5.95	1.72	3.51	0.51	0.00	0.43	0.00	0.43	0.00	1.92
gr17_50_8	9.86	0.76	8.89	0.79	0.36	0.34	0.00	0.36	0.30	0.40	0.00	1.12
gr17_50_9	14.06	0.65	8.14	0.99	3.07	0.56	3.59	0.62	2.77	0.42	0.00	1.69
gr17_50_10	18.91	0.97	0.00	0.81	0.00	0.26	0.00	0.23	0.00	0.26	0.00	6.45
gr21_10_1	0.00	0.40	0.00	0.41	0.00	0.67	0.00	0.69	0.00	0.68	0.00	18.62
gr21_10_2	5.49	2.85	6.05	3.06	2.30	1.37	2.65	1.52	0.00	1.96	0.00	8.53
gr21_10_3	5.05	2.38	5.05	2.45	2.59	1.82	2.55	1.64	0.00	1.00	0.00	11.52
gr21_10_4	0.31	3.46	0.00	2.11	1.56	1.32	1.56	1.34	0.00	0.97	0.00	10.20
gr21_10_5	0.00	0.92	0.00	0.95	0.00	0.12	0.00	0.12	0.00	0.12	0.00	8.49
gr21_10_6	1.92	2.56	1.92	2.56	1.49	1.31	1.49	1.34	0.00	0.46	0.00	7.71
gr21_10_7	12.48	1.95	12.48	1.99	7.77	1.82	7.22	1.87	3.71	3.51	0.00	12.50
gr21_10_8	8.61	2.17	8.61	2.22	7.25	1.24	6.90	1.91	4.03	1.64	0.00	15.72
gr21_10_9	0.00	0.50	0.00	0.53	0.00	0.12	0.00	0.12	0.00	0.12	0.00	11.79
gr21_10_10	0.00	1.18	0.00	1.22	0.00	0.12	0.00	0.13	0.00	0.13	0.00	11.25
gr21_25_1	2.91	2.04	2.91	2.08	0.00	0.64	0.00	0.68	0.00	0.71	0.00	9.20
gr21_25_2	5.44	3.68	5.35	4.47	5.06	1.03	4.73	1.65	0.00	1.95	0.00	7.34
gr21_25_3	12.93	1.88	12.93	1.90	8.96	1.23	8.56	1.08	3.85	2.52	0.00	12.39
gr21_25_4	0.00	0.42	0.00	0.42	0.00	0.10	0.00	0.11	0.00	0.11	0.00	5.96
gr21_25_5	12.63	2.78	12.53	3.60	8.85	1.21	8.32	1.34	4.78	1.34	0.00	23.10
gr21_25_6	5.28	1.90	4.27	3.29	4.95	0.77	5.20	1.02	2.69	1.16	0.00	15.50
gr21_25_7	0.00	0.50	0.00	0.50	0.00	0.46	0.00	0.46	0.00	0.46	0.00	9.36
gr21_25_8	18.25	2.98	18.04	3.84	7.20	2.25	7.75	2.18	6.31	2.01	0.00	21.67
gr21_25_9	0.00	0.57	0.00	0.57	0.00	0.08	0.00	0.08	0.00	0.08	0.00	3.69
gr21_25_10	0.00	0.42	0.00	0.43	0.00	0.09	0.00	0.09	0.00	0.10	0.00	6.22
gr21_50_1	11.36	3.71	11.19	3.79	9.25	0.78	5.76	1.03	2.50	2.58	0.00	8.25
gr21_50_2	17.78	3.93	18.10	4.00	14.28	1.10	14.28	1.15	14.28	1.48	0.00	30.52
gr21_50_3	18.62	3.96	18.65	4.00	3.33	1.60	4.04	1.64	0.00	1.02	0.00	7.74
gr21_50_4	12.33	2.07	12.03	1.74	0.00	1.00	3.11	0.90	0.00	0.67	0.00	10.57
gr21_50_5	15.40	1.77	9.91	2.33	7.73	1.17	6.27	1.35	3.46	2.23	0.00	5.24
gr21_50_6	18.96	2.38	18.43	2.58	7.07	0.95	6.76	1.02	3.42	2.47	0.00	7.33
gr21_50_7	9.86	4.09	10.70	3.45	2.34	0.78	2.03	0.85	0.00	0.71	0.00	7.63
gr21_50_8	11.45	3.49	10.44	4.13	2.56	0.99	2.47	0.96	0.00	0.63	0.00	5.78
gr21_50_9	11.24	1.70	8.55	1.51	8.86	0.83	8.86	0.88	8.86	1.05	0.00	8.80
gr21_50_10	13.33	2.82	12.99	2.70	9.44	1.41	8.20	1.66	3.46	2.62	0.00	11.37

Table B.8
Root node lower bounds: *gr* instances, second part.

Instance	F1		F1 + (12)		F2		F2 + (21)		F2 + (21) + (22)		F3	
	Dev. (%)	Time (seconds)	Dev. (%)	Time (seconds)	Dev. (%)	Time (seconds)	Dev. (%)	Time (seconds)	Dev. (%)	Time (seconds)	Dev. (%)	Time (seconds)
gr48_10_1	5.06	211.26	0.01	686.15	5.04	60.33	1.72	123.43	1.71	336.34	0.98	149.82
gr48_10_2	7.86	466.11	3.99	549.74	6.50	124.86	3.79	183.37	3.29	422.37	0.79	177.09
gr48_10_3	9.78	471.28	5.06	829.72	9.42	51.01	6.38	91.89	5.59	320.18	2.14	210.24
gr48_10_4	9.2	284.93	4.67	821.57	9.48	42.76	6.26	80.48	5.59	386.11	2.77	282.51
gr48_10_5	8.72	529.29	7.13	322.32	8.38	77.30	5.36	143.56	4.35	368.56	1.51	189.48
gr48_10_6	9.01	421.26	3.86	272.60	6.04	49.01	2.86	106.19	2.07	275.41	0.00	41.94
gr48_10_7	5.08	271.69	0.63	279.83	5.33	33.33	2.01	92.31	1.75	424.68	0.00	22.61
gr48_10_8	5.47	230.05	1.77	190.14	5.69	45.91	2.48	198.64	2.00	378.20	0.53	91.35
gr48_10_9	6.73	380.10	2.18	773.43	7.07	42.92	3.76	76.26	3.58	375.60	1.88	224.01
gr48_10_10	5.08	397.71	1.18	838.22	5.22	42.82	1.89	100.30	1.61	342.55	0.78	137.38
gr48_25_1	10.89	312.91	6.66	202.54	9.20	84.62	6.33	127.89	4.68	373.45	1.28	199.82
gr48_25_2	7.57	439.36	4.58	543.73	7.41	67.26	4.64	76.41	3.65	264.52	0.98	113.92
gr48_25_3	14.66	293.35	10.52	521.36	4.79	137.91	2.47	133.09	1.68	277.22	0.00	50.61
gr48_25_4	13.28	522.69	9.91	663.49	10.96	75.00	8.81	59.00	5.55	198.93	0.47	120.07
gr48_25_5	21.62	273.44	18.44	394.15	14.77	109.78	13.55	142.17	8.85	277.28	1.89	228.10
gr48_25_6	16.46	446.68	13.32	180.85	15.50	44.06	13.19	60.91	9.87	259.35	2.34	193.45
gr48_25_7	11.92	240.79	12.49	257.11	7.35	102.58	7.73	81.50	4.51	198.33	1.01	106.02
gr48_25_8	13.42	355.45	9.95	282.72	12.15	52.73	9.09	107.39	7.25	228.75	1.34	154.18
gr48_25_9	16.48	190.07	13.07	1368.84	12.32	71.43	9.76	114.85	7.16	213.78	0.83	131.27
gr48_25_10	19.42	293.33	15.81	783.71	14.37	69.75	11.55	137.84	6.39	340.40	1.01	191.54
gr48_50_1	19.92	230.44	16.82	239.81	15.74	72.93	14.01	78.44	9.31	233.53	0.67	118.30
gr48_50_2	21.55	594.04	19.71	524.20	10.36	64.74	7.93	81.78	4.59	155.09	0.00	21.29
gr48_50_3	17.54	207.74	13.84	605.78	12.91	105.06	9.40	166.23	6.93	189.18	0.00	172.33
gr48_50_4	23.36	269.76	20.71	345.32	12.94	97.13	10.67	100.89	7.18	160.56	0.00	21.07
gr48_50_5	25.01	208.71	21.10	840.29	9.26	112.41	8.60	121.17	4.19	232.83	0.00	19.22
gr48_50_6	19.65	1701.36	19.60	3108.69	6.81	74.25	6.09	72.04	4.39	160.63	0.00	78.63
gr48_50_7	21.38	205.52	17.82	355.09	10.85	86.03	11.29	85.09	8.50	178.64	1.62	147.01
gr48_50_8	25.25	154.13	22.11	304.24	10.70	88.68	9.32	100.09	6.40	141.24	0.00	20.78
gr48_50_9	29.04	269.31	24.58	413.38	7.85	98.42	7.12	95.78	3.60	174.01	0.30	30.71
gr48_50_10	19.10	396.18	15.80	685.31	10.80	118.76	7.87	139.07	5.29	353.82	0.18	111.77

Table C.9
Best Bounds: *burma* instances.

	Rakke et al. (2012)		F1 with (12)				F2 with (21) and (22)				F3		
	Best LB	Best UB	Best LB	Best UB	Tree size	Time (seconds)	Best LB	Best UB	Tree size	Time (seconds)	Opt.	Tree size	Time (seconds)
burma14_10_1	3416	3416	3416	3416	1	0.09	3416	3416	2	0.13	3416	1	0.38
burma14_10_2	3323	3323	3323	3323	1	0.18	3323	3323	1	0.18	3323	1	0.72
burma14_10_3	3323	3323	3323	3323	1	0.16	3323	3323	1	0.13	3323	1	0.41
burma14_10_4	3751	3751	3751	3751	5	0.6	3751	3751	1	0.31	3751	1	0.66
burma14_10_5	3323	3323	3323	3323	1	0.15	3323	3323	1	0.15	3323	1	0.38
burma14_10_6	3323	3323	3323	3323	1	0.24	3323	3323	1	0.13	3323	1	0.65
burma14_10_7	3323	3323	3323	3323	1	0.16	3323	3323	1	0.16	3323	1	0.47
burma14_10_8	3346	3346	3346	3346	1	0.34	3346	3346	1	0.12	3346	1	0.37
burma14_10_9	3416	3416	3416	3416	10	1.54	3416	3416	1	0.23	3416	1	0.52
burma14_10_10	3323	3323	3323	3323	1	0.35	3323	3323	1	0.15	3323	1	0.66
burma14_25_1	4036	4036	4036	4036	119	13.63	4036	4036	1	0.18	4036	1	0.34
burma14_25_2	3465	3465	3465	3465	72	10.51	3465	3465	1	0.20	3465	1	0.37
burma14_25_3	3336	3336	3336	3336	1	0.07	3336	3336	1	0.03	3336	1	0.31
burma14_25_4	3696	3696	3696	3696	68	5.8	3696	3696	8	0.60	3696	1	0.36
burma14_25_5	3346	3346	3346	3346	9	0.95	3346	3346	1	0.15	3346	1	0.45
burma14_25_6	3610	3610	3610	3610	1	0.11	3610	3610	1	0.10	3610	1	0.32
burma14_25_7	3346	3346	3346	3346	1	0.39	3346	3346	1	0.15	3346	1	0.37
burma14_25_8	3371	3371	3371	3371	3	0.29	3371	3371	1	0.24	3371	1	0.45
burma14_25_9	3834	3834	3834	3834	53	6.29	3834	3834	1	0.31	3834	1	0.38
burma14_25_10	3928	3928	3928	3928	40	2.85	3928	3928	1	0.39	3928	1	0.35
burma14_50_1	4412	4412	4412	4412	52	3.9	4412	4412	3	0.23	4412	1	0.32
burma14_50_2	3748	3748	3748	3748	1	0.28	3748	3748	1	0.17	3748	1	0.33
burma14_50_3	3870	3870	3870	3870	1	0.09	3870	3870	1	0.06	3870	1	0.33
burma14_50_4	3323	3323	3323	3323	1	0.15	3323	3323	1	0.05	3323	1	0.31
burma14_50_5	3524	3524	3524	3524	1	0.14	3524	3524	1	0.08	3524	1	0.43
burma14_50_6	3846	3846	3846	3846	13	0.71	3846	3846	1	0.15	3846	1	0.32
burma14_50_7	3408	3408	3408	3408	9	1.14	3408	3408	1	0.23	3408	1	0.37
burma14_50_8	3506	3506	3506	3506	15	1.03	3506	3506	1	0.18	3506	1	0.38
burma14_50_9	4519	4519	4519	4519	30	1.95	4519	4519	1	0.25	4519	1	0.34
burma14_50_10	4467	4467	4467	4467	106	9.21	4467	4467	1	0.23	4467	1	0.32

Table C.10
Best Bounds: *ulysses* instances.

	Rakke et al. (2012)		F1 with (12)				F2 with (21) and (22)				F3		
	Best LB	Best UB	Best LB	Best UB	Tree size	Time (seconds)	Best LB	Best UB	Tree size	Time (seconds)	Opt.	Tree size	Time (seconds)
ulysses16_10_1	6859	6859	6859	6859	1	0.47	6859	6859	1	0.21	6859	1	33.88
ulysses16_10_2	6859	6859	6859	6859	1	0.51	6859	6859	1	0.25	6859	1	46.83
ulysses16_10_3	6859	6859	6859	6859	1	0.29	6859	6859	1	0.26	6859	1	72.6
ulysses16_10_4	6859	6859	6859	6859	1	0.4	6859	6859	1	0.22	6859	1	33.04
ulysses16_10_5	6859	6859	6859	6859	1	0.32	6859	6859	1	0.24	6859	1	60.21
ulysses16_10_6	6951	6951	6951	6951	5	0.74	6951	6951	1	0.39	6951	1	32.58
ulysses16_10_7	6859	6859	6859	6859	1	0.5	6859	6859	1	0.34	6859	1	62.46
ulysses16_10_8	6859	6859	6859	6859	1	0.5	6859	6859	1	0.21	6859	1	40.66
ulysses16_10_9	6859	6859	6859	6859	1	0.46	6859	6859	1	0.34	6859	1	75.11
ulysses16_10_10	6859	6859	6859	6859	1	0.59	6859	6859	1	0.36	6859	1	48.59
ulysses16_25_1	6890	6890	6890	6890	11	1.76	6890	6890	1	0.57	6890	1	49.57
ulysses16_25_2	6859	6859	6859	6859	1	0.29	6859	6859	1	0.32	6859	1	3.98
ulysses16_25_3	6859	6859	6859	6859	1	0.27	6859	6859	1	0.38	6859	1	21.95
ulysses16_25_4	7401	7401	7401	7401	22	3.68	7401	7401	1	0.43	7401	1	3.52
ulysses16_25_5	7671	7671	7671	7671	92	21.71	7671	7671	1	0.48	7671	1	11.1
ulysses16_25_6	7029	7029	7029	7029	1	0.62	7029	7029	1	0.32	7029	1	10.16
ulysses16_25_7	7446	7446	7446	7446	10	1.93	7446	7446	1	0.71	7446	1	9.81
ulysses16_25_8	6859	6859	6859	6859	1	0.75	6859	6859	1	0.27	6859	1	43.05
ulysses16_25_9	6859	6859	6859	6859	1	0.26	6859	6859	1	0.16	6859	1	11.32
ulysses16_25_10	7781	7781	7781	7781	204	77.53	7781	7781	24	2.87	7781	1	21.31
ulysses16_50_1	7264	7264	7264	7264	7	1.3	7264	7264	1	0.48	7264	1	2.09
ulysses16_50_2	7715	7715	7715	7715	8	1.3	7715	7715	1	0.28	7715	1	2.6
ulysses16_50_3	9612	9612	9612	9612	2	0.24	9612	9612	1	0.08	9612	1	1.2
ulysses16_50_4	7313	7313	7313	7313	19	2.45	7313	7313	1	0.31	7313	1	1.26
ulysses16_50_5	6909	6909	6909	6909	1	0.86	6909	6909	1	0.19	6909	1	9.93
ulysses16_50_6	7301	7301	7301	7301	6	1.16	7301	7301	1	0.25	7301	1	3.66
ulysses16_50_7	8118	8118	8118	8118	208	37.42	8118	8118	12	1.02	8118	1	3.06
ulysses16_50_8	7065	7065	7065	7065	1	0.1	7065	7065	1	0.05	7065	1	2.4
ulysses16_50_9	6900	6900	6900	6900	4	1.22	6900	6900	1	0.27	6900	1	11.81
ulysses16_50_10	7706	7706	7706	7706	18	1.78	7706	7706	1	0.29	7706	1	7.97
ulysses22_10_1	7013	7013	7013	7013	3	4.93	7013	7013	1	0.98	7013	1	35.76
ulysses22_10_2	7013	7013	7013	7013	1	1.71	7013	7013	1	0.83	7013	1	26.54
ulysses22_10_3	7013	7013	7013	7013	1	1.21	7013	7013	1	0.57	7013	1	28.06
ulysses22_10_4	7013	7013	7013	7013	3	4.99	7013	7013	1	0.82	7013	1	19.77
ulysses22_10_5	7013	7013	7013	7013	1	1.14	7013	7013	1	1.23	7013	1	39.26
ulysses22_10_6	7250	7250	7250	7250	16	8.28	7250	7250	1	1.12	7250	1	40.55
ulysses22_10_7	7246	7246	7147	7246	2169	7200.13	7246	7246	87	39.58	7246	1	40.2
ulysses22_10_8	7181	7181	7181	7181	43	19.89	7181	7181	1	1.21	7181	1	55.88
ulysses22_10_9	7047	7047	7047	7047	1	1.11	7047	7047	1	0.95	7047	1	18.25
ulysses22_10_10	7087	7087	7087	7087	34	24.81	7087	7087	7	4.42	7087	1	17.92
ulysses22_25_1	7083	7083	7083	7083	22	15.56	7083	7083	3	2.90	7083	1	30.63
ulysses22_25_2	7415	7415	**7232.17**	**7444**	2987	7200.06	7415	7415	195	69.05	7415	1	19.25
ulysses22_25_3	8177	8177	**7870.54**	8177	3899	7200.19	8177	8177	760	173.82	8177	1	21.95
ulysses22_25_4	7385	7385	**7249.00**	**7415**	2984	7200.05	7385	7385	35	26.12	7385	1	28.7
ulysses22_25_5	7449	7449	**7250.26**	**7599**	3425	7200.03	7449	7449	20	9.52	7449	1	23.58
ulysses22_25_6	7589	7589	**7347.00**	**7826**	5308	7200.15	7589	7589	51	20.47	7589	1	32.37
ulysses22_25_7	7729	7729	**7271.44**	**7809**	3724	7200.12	7729	7729	108	40.37	7729	1	23.91
ulysses22_25_8	7123	7123	7123	7123	156	96.87	7123	7123	1	1.26	7123	1	17.45
ulysses22_25_9	7176	7176	7176	7176	3	4.36	7176	7176	1	1.74	7176	1	27.08
ulysses22_25_10	7961	7961	7961	7961	3	2.31	7961	7961	1	1.07	7961	1	22.77
ulysses22_50_1	8290	8290	**7757.12**	**8455**	4749	7200.11	8290	8290	261	84.87	8290	1	24.18
ulysses22_50_2	7538	7538	7538	7538	2057	6256.13	7538	7538	61	30.76	7538	1	16.58
ulysses22_50_3	**8641.46**	**8919**	**8145.46**	**8901**	6559	7200.05	8833	8833	375	98.28	8833	1	21.75
ulysses22_50_4	**8829.07**	–	9324	9324	143	103.22	9324	9324	1	2.29	9324	1	38.53
ulysses22_50_5	8284	8284	8284	8284	2694	3340.3	8284	8284	25	7.11	8284	1	46.11
ulysses22_50_6	7570	7570	7570	7570	1126	1525.42	7570	7570	1	2.94	7570	1	10.6
ulysses22_50_7	7897	7897	**7748.13**	**7897**	4395	7200.04	7897	7897	1	1.70	7897	1	25.41
ulysses22_50_8	9558	9558	**9177.75**	**9577**	5911	7200.03	9558	9558	125	34.68	9558	1	20.68
ulysses22_50_9	**8453.35**	–	**8296.29**	**9316**	7419	7200	9021	9021	795	253.16	9021	1	48.15
ulysses22_50_10	7941	7941	**7754.85**	7941	2706	7200.08	7941	7941	233	65.26	7941	1	15.13

Table C.11
Best Bounds: *fri* instances.

	Rakke et al. (2012)		F1 with (12)				F2 with (21) and (22)				F3		
	Best LB	Best UB	Best LB	Best UB	Tree size	Time (seconds)	Best LB	Best UB	Tree size	Time (seconds)	Opt.	Tree size	Time (seconds)
fri26_10_1	937	937	937	937	1	3.51	937	937	1	1.67	937	1	11.99
fri26_10_2	937	937	937	937	1	4.2	937	937	1	1.72	937	1	11.35
fri26_10_3	1009	1009	1009	1009	186	459	1009	1009	13	16.39	1009	1	14.54
fri26_10_4	955	955	955	955	90	133.25	955	955	12	8.50	955	1	12.61
fri26_10_5	997	997	997	997	483	2976.6	997	997	1	9.39	997	1	21.95
fri26_10_6	937	937	937	937	1	4.88	937	937	1	1.29	937	1	8.54
fri26_10_7	1039	1039	**976.62**	**1062**	2488	7200.14	1039	1039	292	287.18	1039	1	14.24
fri26_10_8	953	953	953	953	11	21.59	953	953	1	5.84	953	1	8.33
fri26_10_9	937	937	937	937	1	2.3	937	937	1	2.04	937	1	11.18
fri26_10_10	937	937	937	937	1	3.86	937	937	1	1.87	937	1	9.98
fri26_25_1	1055	1055	**1036.14**	**1076**	1537	7200.13	1055	1055	15	11.96	1055	1	14.7
fri26_25_2	1201	1201	1201	1201	28	30.09	1201	1201	11	15.17	1201	1	26.49
fri26_25_3	1139	1139	1139	1139	294	778.22	1139	1139	20	10.88	1139	1	24.34
fri26_25_4	**1152.76**	–	**1098.29**	**1285**	4118	7200.13	1233	1233	75	68.20	1233	1	24.35
fri26_25_5	1017	1017	**990.00**	**1067**	2649	7200.06	1017	1017	41	42.68	1017	1	14.96
fri26_25_6	**1135.84**	–	**1100.86**	**1172**	2875	7200.06	1172	1172	54	49.19	1172	1	14.79
fri26_25_7	1101	1101	**994.73**	**1114**	2332	7200.1	1101	1101	79	62.61	1101	1	19.01
fri26_25_8	955	955	955	955	30	27.09	955	955	6	6.11	955	1	6.46
fri26_25_9	1081	1081	**996.00**	**1086**	3356	7200.1	1081	1081	98	89.52	1081	1	10.24
fri26_25_10	1093	1093	**1090.50**	1093	1822	7200.19	1093	1093	145	114.21	1093	1	9.22
fri26_50_1	**1150.65**	–	**1138.50**	**1367**	7433	7200.01	1273	1273	44	28.14	1273	1	16.64
fri26_50_2	1045	1045	**983.85**	**1075**	3426	7200.12	1045	1045	57	49.85	1045	1	22.21
fri26_50_3	1035	1035	**1014.70**	1035	2540	7200.09	1035	1035	12	20.56	1035	1	12.52
fri26_50_4	1185	1185	**1117.97**	**1206**	5664	7200.12	1185	1185	31	15.11	1185	1	12.13
fri26_50_5	**1144.26**	–	**1120.77**	1185	4327	7200.12	1185	1185	1	2.28	1185	1	12.57
fri26_50_6	1158	1158	1158	1158	883	2144.05	1158	1158	26	12.44	1158	1	9.9
fri26_50_7	**1119.01**	**1162**	**1126.34**	**1152**	3910	7200.1	1150	1150	1	5.81	1150	1	14.74
fri26_50_8	**1174.96**	–	**1437.92**	1441	3796	7200.03	1441	1441	41	18.29	1441	1	22.36
fri26_50_9	**1165.15**	–	**1232.28**	**1279**	5320	7200.02	1267	1267	35	23.08	1267	1	28.57
fri26_50_10	1048	1048	**1014.53**	1048	1911	7200.19	1048	1048	271	192.33	1048	1	11.96

Table C.12
Best Bounds: *bayg* instances.

	Rakke et al. (2012)		F1 with (12)				F2 with (21) and (22)				F3		
	Best LB	Best UB	Best LB	Best UB	Tree size	Time (seconds)	Best LB	Best UB	Tree size	Time (seconds)	Opt.	Tree size	Time (seconds)
bayg29_10_1	1610	1610	1610	1610	3	19.05	1610	1610	1	4.90	1610	1	10.98
bayg29_10_2	1654	1654	**1644.67**	1654	552	7200.11	1654	1654	39	82.42	1654	1	9.9
bayg29_10_3	1753	1753	1753	1753	61	308.48	1753	1753	18	34.07	1753	1	11.73
bayg29_10_4	1622	1622	1622	1622	39	59.36	1622	1622	1	3.26	1622	1	8.32
bayg29_10_5	1645	1645	1645	1645	249	1985.4	1645	1645	71	57.32	1645	1	12.59
bayg29_10_6	1622	1622	1622	1622	65	359.66	1622	1622	6	16.01	1622	1	10.16
bayg29_10_7	1833	1833	1833	1833	181	284.53	1833	1833	13	29.68	1833	1	11.08
bayg29_10_8	2114	2114	2114	2114	1	4.1	2114	2114	1	5.30	2114	1	17.69
bayg29_10_9	1628	1628	1628	1628	74	93.02	1628	1628	6	18.41	1628	1	14.96
bayg29_10_10	1655	1655	1655	1655	643	6081.76	1655	1655	61	105.03	1655	1	13.51
bayg29_25_1	**1998.33**	–	**1940.75**	**2129**	1531	7200.15	2027	2027	68	89.09	2027	1	10.53
bayg29_25_2	1655	1655	1655	1655	546	4188.57	1655	1655	48	105.54	1655	1	14.43
bayg29_25_3	1827	1827	**1682.57**	**2012**	2779	7200.03	1827	1827	337	489.54	1827	1	16.52
bayg29_25_4	**1766.08**	–	**1643.08**	**1921**	2230	7200.43	1799	1799	1113	1335.08	1799	1	10.17
bayg29_25_5	1709	1709	1709	1709	449	4214.29	1709	1709	43	59.51	1709	1	15.12
bayg29_25_6	1841	1841	1841	1841	45	52.88	1841	1841	14	27.69	1841	1	9.79
bayg29_25_7	1805	1805	**1663.50**	**1965**	2747	7200.23	1805	1805	196	340.48	1805	1	9.08
bayg29_25_8	1718	1718	**1654.67**	**1823**	1882	7200.06	1718	1718	107	177.38	1718	1	10.97
bayg29_25_9	1683	1683	**1648.61**	**1698**	1253	7200.14	1683	1683	54	99.25	1683	1	8.05
bayg29_25_10	1862	1862	1862	1862	1	4.34	1862	1862	1	0.81	1862	1	6.99
bayg29_50_1	**1825.44**	–	**1699.30**	**2105**	3030	7200.15	1928	1928	314	280.36	1928	1	14.16
bayg29_50_2	**2032.96**	–	**2080.47**	**2456**	7101	7200.03	2255	2255	20	23.19	2255	1	11.27
bayg29_50_3	**1991.82**	–	**1849.78**	**2233**	3361	7200.09	2093	2093	123	137.42	2093	1	11.04
bayg29_50_4	**1924.07**	–	**1790.00**	**2054**	2661	7200.08	2019	2019	679	546.84	2019	1	9.18
bayg29_50_5	1785	1785	**1734.45**	**1842**	1772	7200.05	1785	1785	79	106.53	1785	1	8.65
bayg29_50_6	**2055.74**	–	**2113.94**	**2561**	6854	7200	2340	2340	496	326.92	2340	1	11.19
bayg29_50_7	**1955.11**	–	**2221.70**	**2576**	5509	7200.08	2400	2400	308	246.81	2400	1	11.32
bayg29_50_8	**1878.70**	–	**1865.63**	**2405**	5935	7200.08	2204	2204	191	155.77	2204	1	34.68
bayg29_50_9	**1887.86**	–	**1819.50**	**2050**	3792	7200.28	1987	1987	997	743.40	1987	1	12.99
bayg29_50_10	**1876.04**	**1947**	1899	1899	614	1876.37	1899	1899	12	13.72	1899	1	10.16

Table C.13
Best Bounds: *gr* instances, first part.

	Rakke et al. (2012)		F1 with (12)				F2 with (21) and (22)				F3		
	Best LB	Best UB	Best LB	Best UB	Tree size	Time (seconds)	Best LB	Best UB	Tree size	Time (seconds)	Opt.	Tree size	Time (seconds)
gr17_10_1	2153	2153	2153	2153	17	3.71	2153	2153	1	0.23	2153	1	21.86
gr17_10_2	2165	2165	2165	2165	1	0.32	2165	2165	1	0.20	2165	1	28.69
gr17_10_3	2085	2085	2085	2085	1	0.48	2085	2085	1	0.39	2085	1	34.6
gr17_10_4	2590	2590	2590	2590	1	0.19	2590	2590	1	0.29	2590	1	18.36
gr17_10_5	2085	2085	2085	2085	1	0.54	2085	2085	1	0.36	2085	1	23.95
gr17_10_6	2085	2085	2085	2085	1	0.46	2085	2085	1	0.27	2085	1	24.9
gr17_10_7	2085	2085	2085	2085	1	0.41	2085	2085	1	0.44	2085	1	26.33
gr17_10_8	2085	2085	2085	2085	1	0.4	2085	2085	1	0.51	2085	1	2.71
gr17_10_9	2085	2085	2085	2085	1	1.11	2085	2085	1	0.38	2085	1	25.06
gr17_10_10	2085	2085	2085	2085	1	0.53	2085	2085	1	0.33	2085	1	46.16
gr17_25_1	2265	2265	2265	2265	229	62.83	2265	2265	2	0.51	2265	1	3.18
gr17_25_2	2505	2505	2505	2505	986	571.98	2505	2505	20	2.17	2505	1	16.48
gr17_25_3	2270	2270	2270	2270	14	2.61	2270	2270	1	0.34	2270	1	4.3
gr17_25_4	2103	2103	2103	2103	6	2.03	2103	2103	1	0.32	2103	1	20.1
gr17_25_5	2088	2088	2088	2088	5	1.44	2088	2088	1	0.47	2088	1	22.16
gr17_25_6	2160	2160	2160	2160	55	8.99	2160	2160	1	0.24	2160	1	9.34
gr17_25_7	2085	2085	2085	2085	1	0.55	2085	2085	1	0.34	2085	1	15.93
gr17_25_8	2088	2088	2088	2088	1	0.32	2088	2088	1	0.23	2088	1	10.47
gr17_25_9	2138	2138	2138	2138	1	1.32	2138	2138	1	0.47	2138	1	1.96
gr17_25_10	2675	2675	2675	2675	113	25.98	2675	2675	1	0.75	2675	1	8.25
gr17_50_1	2743	2743	2743	2743	609	177.25	2743	2743	2	0.57	2743	1	9.46
gr17_50_2	2216	2216	2216	2216	85	14.05	2216	2216	1	0.26	2216	1	6.67
gr17_50_3	3000	3000	3000	3000	20	2.34	3000	3000	2	0.35	3000	1	1.77
gr17_50_4	2946	2946	2946	2946	20	2.72	2946	2946	1	0.36	2946	1	4.73
gr17_50_5	2205	2205	2205	2205	37	5.56	2205	2205	1	0.67	2205	1	19.37
gr17_50_6	2579	2579	2579	2579	1	0.24	2579	2579	1	0.31	2579	1	2.63
gr17_50_7	2812	2812	2812	2812	37	5.57	2812	2812	1	0.43	2812	1	2.01
gr17_50_8	3014	3014	3014	3014	67	6.06	3014	3014	3	0.40	3014	1	1.14
gr17_50_9	3454	3454	3454	3454	157	28.05	3454	3454	6	0.49	3454	1	1.73
gr17_50_10	2134	2134	2134	2134	2	0.81	2134	2134	1	0.26	2134	1	6.52
gr21_10_1	2707	2707	2707	2707	1	0.4	2707	2707	1	0.68	2707	1	18.77
gr21_10_2	3002	3002	3002	3002	11	5.94	3002	3002	1	1.95	3002	1	8.58
gr21_10_3	2851	2851	2851	2851	124	86.63	2851	2851	1	0.99	2851	1	11.62
gr21_10_4	2760	2760	2760	2760	1	2.04	2760	2760	1	0.97	2760	1	10.25
gr21_10_5	2707	2707	2707	2707	1	0.92	2707	2707	1	0.12	2707	1	8.56
gr21_10_6	2760	2760	2760	2760	69	46.02	2760	2760	1	0.46	2760	1	7.76
gr21_10_7	3093	3093	**2960.64**	**3108**	3245	7200.11	3093	3093	40	15.65	3093	1	12.58
gr21_10_8	2962	2962	2962	2962	650	1204.29	2962	2962	23	6.67	2962	1	15.88
gr21_10_9	2787	2787	2787	2787	1	0.5	2787	2787	1	0.13	2787	1	11.9
gr21_10_10	2707	2707	2707	2707	1	1.19	2707	2707	1	0.13	2707	1	11.32
gr21_25_1	2788	2788	2788	2788	20	8.14	2788	2788	1	0.70	2788	1	9.32
gr21_25_2	2946	2946	2946	2946	229	162.87	2946	2946	1	1.94	2946	1	7.43
gr21_25_3	3109	3109	3109	3109	2056	3907.56	3109	3109	9	3.27	3109	1	12.53
gr21_25_4	2707	2707	2707	2707	1	0.42	2707	2707	1	0.11	2707	1	6.01
gr21_25_5	3159	3159	3159	3159	1584	1637.24	3159	3159	18	4.57	3159	1	23.31
gr21_25_6	3159	3159	3159	3159	119	45.6	3159	3159	13	3.29	3159	1	15.72
gr21_25_7	2921	2921	2921	2921	1	0.51	2921	2921	1	0.46	2921	1	9.45
gr21_25_8	3421	3421	**3272.65**	3421	4801	7200.04	3421	3421	44	9.69	3421	1	21.77
gr21_25_9	2709	2709	2709	2709	1	0.57	2709	2709	1	0.08	2709	1	3.74
gr21_25_10	2707	2707	2707	2707	1	0.42	2707	2707	1	0.09	2707	1	6.26
gr21_50_1	3115	3115	3115	3115	2738	6884.75	3115	3115	21	7.28	3115	1	8.34
gr21_50_2	4041	4041	4041	4041	4397	5315.73	4041	4041	19	5.20	4041	1	30.7
gr21_50_3	3892	3892	3892	3892	1448	745.36	3892	3892	1	1.02	3892	1	7.82
gr21_50_4	3570	3570	3570	3570	313	134.06	3570	3570	2	0.67	3570	1	10.64
gr21_50_5	4132	4132	**4116.98**	**4155**	3271	7200.04	4132	4132	34	11.09	4132	1	5.32
gr21_50_6	3417	3417	**3368.96**	**3424**	5209	7200.12	3417	3417	36	9.21	3417	1	7.43
gr21_50_7	4249	4249	4249	4249	130	45.3	4249	4249	1	0.70	4249	1	7.71
gr21_50_8	3296	3296	3296	3296	887	445.02	3296	3296	1	0.62	3296	1	5.85
gr21_50_9	4186	4186	4186	4186	1838	1448.02	4186	4186	12	1.57	4186	1	8.88
gr21_50_10	3483	3483	3483	3483	2759	4236.61	3483	3483	21	7.64	3483	1	11.47

Table C.14
Best Bounds: *gr* instances, second part.

	Rakke et al. (2012)		F1 with (12)				F2 with (21) and (22)				F3		
	Best LB	Best UB	Best LB	Best UB	Tree size	Time (seconds)	Best LB	Best UB	Tree size	Time (seconds)	Opt.	Tree size	Time (seconds)
gr48_10_1	5046	5046	5046	5046	14	716.242	5046	5046	22	1186.49	5046	49	813.29
gr48_10_2	5542	5542	**5348.75**	**10022**	270	7200.33	**5400.02**	**6018**	332	7204.52	5542	15	341.27
gr48_10_3	**5150.54**	**5166.16**	**5039.00**	**–**	206	7200.34	**5075.9**	**5484**	390	7200.02	5300	185	3314.02
gr48_10_4	**5199.8**	–	**5046.00**	**8692**	251	7200.19	**5049.68**	**5443**	359	7203.32	5293	359	7057.36
gr48_10_5	**5596.14**	–	**5287.55**	**10384**	144	7200.33	**5486.15**	**5784**	565	7205.46	5679	29	496.29
gr48_10_6	5610	5610	**5487.20**	**–**	257	7200.07	5610	5610	186	4339.84	5610	1	41.04
gr48_10_7	5063	5063	**5046.33**	**5944**	157	7200.41	**5029.47**	**5584**	312	7200.02	5063	1	22.79
gr48_10_8	5103	5103	**5076.50**	**5103**	121	7200.66	5103	5103	177	4508.85	5103	15	188.77
gr48_10_9	5153	5153	**5046.09**	**6236**	220	7200.3	**5025.44**	**5784**	249	7208.20	5153	51	892.87
gr48_10_10	5055	5055	**5031.17**	**–**	108	7200.04	5055	5055	45	1970.82	5055	23	359.47
gr48_25_1	**5445.21**	**5771**	**5161.65**	**9234**	197	7200.29	**5333.38**	**5633**	438	7202.06	5524	89	1073.43
gr48_25_2	**5567.52**	–	**5629.48**	**7850**	221	7200.02	**5747.21**	**6069**	608	7200.02	5895	29	361.9
gr48_25_3	**5328.93**	–	**5182.00**	**–**	168	7200.32	**5736.44**	**5759**	591	7203.62	5754	1	47.85
gr48_25_4	**5253.55**	–	**5052.39**	**–**	361	7200.24	**5341.41**	**5705**	485	7200.03	5588	5	126.05
gr48_25_5	**5253.54**	–	**5036.13**	**10911**	302	7200.16	**5690.94**	**7237**	666	7200.02	6159	123	1793.96
gr48_25_6	**5239.1**	–	**5034.00**	**10930**	316	7200.08	**5260.98**	**6540**	514	7202.55	5760	161	3053.47
gr48_25_7	**5315.58**	–	**5348.78**	**9937**	402	7200.2	**5804.83**	**6030**	789	7202.86	5955	13	172.08
gr48_25_8	**5238.68**	–	**5029.00**	**8877**	340	7200.27	**5172.39**	**7088**	591	7204.34	5562	45	1070.86
gr48_25_9	**5215.81**	–	**5059.50**	**8593**	261	7200.05	**5405.91**	**6398**	483	7201.16	5792	7	184.24
gr48_25_10	**5245.96**	–	**5085.50**	**8212**	422	7200.32	**5644.65**	**6668**	545	7200.02	6014	27	730.82
gr48_50_1	**5285.12**	–	**5094.85**	**10706**	496	7200.08	**5629.73**	**6527**	715	7200.03	6096	7	157.47
gr48_50_2	**5247.71**	–	**5694.77**	**11156**	373	7200.43	**6416.57**	**6678**	909	7200.03	6629	1	21.44
gr48_50_3	**5262.54**	–	**5104.29**	**10614**	433	7200.2	**5565.93**	**6226**	670	7200.14	5896	3	132.45
gr48_50_4	**5368.73**	–	**5125.00**	**10322**	623	7200.27	**6045.54**	**6647**	946	7200.06	6404	1	20.75
gr48_50_5	**5422.02**	–	**5237.00**	**8889**	470	7200.26	**6593.5**	**6694**	711	7201.24	6617	1	19.41
gr48_50_6	**6096.34**	–	**6921.32**	**9799**	246	7200.66	**8381.52**	**8569**	1291	7200.21	8533	1	66.09
gr48_50_7	**5298.52**	–	**5099.00**	**8320**	492	7200.37	**5741.68**	**6473**	939	7202.60	6166	109	1520.1
gr48_50_8	**5382.83**	–	**5122.00**	**10388**	516	7200.28	**6286.1**	6535	1164	7201.92	6535	1	20.93
gr48_50_9	**5319.51**	–	**5430.39**	**11797**	838	7200.13	**7000.3**	**7393**	1352	7200.59	7150	7	42.73
gr48_50_10	**5467.79**	–	**5345.50**	**12305**	467	7200.01	**6089.21**	**6419**	644	7200.01	6331	3	112.13

References

Abeledo, H., Fukasawa, R., Pessoa, A. Uchoa, & E. (2013). The time dependent traveling salesman problem: Polyhedra and algorithm. *Mathematical Programming Computation, 5*, 27–55.

Balas, E., & Fischetti, M. (2004). Polyhedral theory for the asymmetric traveling salesman problem. In G. Gutin, A. Punnen, D.-Z. Du, & P. Pardalos (Eds.), *The traveling salesman problem and its variations. Combinatorial optimization* (pp. 117–168). US: Springer.

Baldacci, R., Mingozzi, A., & Roberti, R. (2011). New route relaxation and pricing strategies for the vehicle routing problem. *Operations Research, 59*, 1269–1283.

Dantzig, G., Fulkerson, R., & Johnson, S. (1954). Solution of a large-scale traveling-salesman problem. *Operations Research, 2*, 393–410.

Fox, K., Gavish, B., & Graves, S. (1980). An n-constraint formulation of the (time-dependent) traveling salesman problem. *Operations Research, 28*, 1018–1021.

Irnich, S., & Villeneuve, D. (2006). The shortest-path problem with resource constraints and k-cycle elimination for $k \geq 3$. *INFORMS Journal on Computing, 18*, 391–406.

Keha, A., Khowala, K., & Fowler, J. (2009). Mixed integer programming formulations for single machine scheduling problems. *Computers & Industrial Engineering, 56*, 357–367.

Lysgaard, J. (2003). *CVRPSEP: A package of separation routines for the capacitated vehicle routing problem. Working paper*.

Miller, C., Tucker, A., & Zemlin, R. (1960). Integer programming formulation of traveling salesman problems. *Journal of the ACM, 7*, 326–329.

Pessoa, A., Poggi de Aragão, M., Uchoa, E. (2008). *The vehicle routing problem: Latest advances and new challenges* (pp. 297–325). Ch. Robust BCP algorithms for Vehicle Routing Problems: Springer US.

Pessoa, A., Uchoa, E., Poggi, M., & Rodrigues, R. (2010). Exact algorithm over an arc-time-indexed formulation for parallel machine scheduling problems. *Mathematical Programming Computation, 2*, 259–290.

Rakke, J., Christiansen, M., Fagerholt, K., & Laporte, G. (2012). The traveling salesman problem with draft limits. *Computers & Operations Research, 39*, 2161–2167.

Roberti, R., & Toth, P. (2012). Models and algorithms for the asymmetric traveling salesman problem: An experimental comparison. *EURO Journal of Transportation and Logistics, 1*, 113–133.

Subramanian, A., Uchoa, E., Pessoa, A. A., & Ochi, L. S. (2013). Branch-cut-and price for the vehicle routing problem with simultaneous pickup and delivery. *Optimization Letters, 7*, 1569–1581.